

Topological effect on order-disorder transitions in U(1) sigma models

Ryuichi Shindou and Pengwei Zhao

International Center for Quantum Materials, Peking University, Beijing 100871, China

(Dated: April 1, 2025)

U(1) non-linear sigma model (NLSM) with a one-dimensional (1D) Berry phase is studied by a renormalization group theory. Order-disorder transition in U(1) NLSMs in $D (\geq 2)$ -dimensional space ($d + 1$ -dimensional spacetime; $d \geq 1$) is instigated by the proliferation of vortex excitations, where the 1D Berry phase term confers finite phase factors upon those vortex excitations that have finite projection in a subspace complementary to a topological direction with the 1D Berry phase. Due to a destructive interference effect caused by the phase factors, a partition function near the order-disorder transition point can be dominated by vortex excitations polarized along the topological direction with the Berry phase. The proliferation of the polarized vortex excitations helps to develop an extremely anisotropic correlation of the order parameter, which has a divergent correlation length along the topological direction with the Berry phase, and a finite correlation length along the other directions. In order to explore such a possibility in $D = 3$, we develop a perturbative renormalization group theory of a 3D model of vortex loops, in which loop segments interact via a $1/r$ Coulomb interaction, and the 1D Berry phase confers the phase factor upon each vortex loop. We derive renormalization group (RG) equations among vortex-loop fugacity, Berry phase term, and the Coulomb potential. The RG equations analyzed with approximations show that a characteristic size of the vortex loop along the topological direction becomes anomalously large near an order-disorder transition point, while the characteristic loop size within the other directions remains finite. Utilizing a duality mapping to a lattice model of a type-II superconductor under a magnetic field, we also argue that a global phase diagram of the 3D U(1) sigma model with 1D Berry phase should have an intermediate quasi-disorder phase between ordered and disorder phases.

I. INTRODUCTION

An U(1) nonlinear sigma model (NLSM) with a Berry phase term is an effective continuum model that describes phase transitions associated with spontaneous symmetry breaking of a global U(1) symmetry,

$$Z = \int D\theta(x) e^{-\int d^D x \left\{ \frac{1}{2T} \nabla\theta(x) \cdot \nabla\theta(x) + i\chi \nabla_0\theta(x) \right\}}, \quad (1)$$

with $x \equiv (x_1, \dots, x_d, x_0)^T$, $D \equiv d + 1$, and a U(1) phase variable $\theta(x) \in [0, 2\pi)$. Relevant phase transitions and physical systems include superfluid systems [1–5], three-dimensional (3D) type-II superconductors under an external magnetic field [6–14], and disordered systems of free particles in Hermitian chiral symmetry classes [15–29]. The NLSM in $D = d + 1$ dimension represents a zero-temperature partition function of d -dimensional superfluid systems where superfluid phase $\theta(x)$ fluctuates in space $x_\perp \equiv (x_1, \dots, x_d)$ and imaginary time x_0 , while superfluid amplitude is constrained around a finite value by certain physical means. Thereby, the Berry phase term χ along the imaginary time direction originates from a quantum-mechanical commutation relation between superfluid amplitude and phase [30, 31]. Previous studies on the superfluid systems discovered Bose glass [32–34] and Griffiths [35–39] phases. In these glassy phases, the superfluid correlation time is divergent, while the superfluid correlation length remains finite.

A dual lattice model of the U(1) NLSM in $D = 3$ portrays magnetostatics of the 3D type-II superconductors in the x_1 - x_2 - x_0 space, where the order and disorder phases of the U(1) NLSM describe normal

(“Maxwell”) and superconducting (“Meissner”) phases, respectively [6–9, 11, 30, 40, 41]. Thereby, the Berry phase term χ in the NLSM originates from an external magnetic field applied along the x_0 direction in the superconductors. The dual description identifies a correlation function of the U(1) phase variable $e^{i\theta(x)}$ in the NLSM with a correlation function of magnetic monopole fields in the superconductors. It has been known that the type-II superconductors under the magnetic field have novel mixed phases, such as 3D vortex lattice or vortex liquid phases. In these mixed phases, the monopole-field correlation function has a divergent correlation length along the field (x_0) direction, and a finite correlation length along the others (x_1 and x_2) directions.

The U(1) NLSM in $D = d + 1$ dimension is also relevant to the D -dimensional Anderson transition of disordered Hermitian in the chiral symmetric classes [15–17, 24, 25]. The ordered and disorder phases in the U(1) NLSM correspond to metal and localized phases in the Anderson transition of the chiral symmetric models, respectively. Thereby, the Berry phase term χ originates from one-dimensional (1D) band topology along the x_0 direction in the chiral symmetric Hamiltonians [19, 20, 26, 27], and such Hamiltonians can be realized in semimetal models [21, 28, 29]. Recent numerical studies on the semimetal models in $D = 2, 3$ clarified that the 1D topology universally induces a quasi-localized phase between metal and Anderson localized phases [28, 29]. In the quasi-localized phase, an exponential localization length is divergent along the 1D topological (x_0) direction, while it is finite along the other directions.

A recent theory discussed the universal emergence of the quasi-localized phase in the 2D disordered chiral sym-

metric systems through the lens of the NLSM with the 1D Berry phase term [29]. The 2D Anderson transition in the chiral symmetry classes is driven by a spatial proliferation of vortex-antivortex pairs associated with a U(1) phase $\theta(x)$ degree of freedom of a Q -field in a matrix-formed NLSM [17, 42–45]. The 1D band topology along the x_0 direction confers a complex phase factor upon such pairs, and the phase for each pair is proportional to a projected length m_1 of a dipole vector $m \equiv (m_0, m_1)$ of the pair along the x_1 direction [18, 19, 29, 31]. In a partition function, such phase factor induces destructive interference among those pairs with a finite angle against the x_0 axis and different dipole lengths $|m|$. Consequently, the partition function near the transition point is expected to be dominated by vortex-antivortex pairs polarized along the x_0 axis ($m_1 = 0$). An introduction of a vortex-antivortex pair generally adds on a relative U(1) phase $\delta\theta(y, z) \equiv \theta(y) - \theta(z)$ between two spatial points, y and z . Such add-on phase winds up the 2π phase when the dipole length $|m|$ of the pair with a perpendicular geometry $m \perp y - z$ changes from 0 to ∞ . For the other geometry ($m \parallel y - z$), the additive phase does not. This indicates that the proliferation of the polarized pairs results in an emergence of the quasi-localized phase where a correlation function $\langle e^{i\theta(x) - i\theta(y)} \rangle$ of the U(1) phase has a divergent correlation length along the topological (x_0) direction, and finite correlation length along the other (x_1) direction. To uphold this physical picture, the theory further studied a U(N) NLSM for chiral unitary classes with the 1D weak topology, and derived RG equations among vortex fugacity, 1D topology parameter, and conductivities. The RG equations have a stable fixed point, and a stable fixed region. The stable point is characterized by divergent vortex fugacity, *finite* conductivity along the topological (x_0) direction, and vanishing conductivity along the other (x_1) direction. The stable region is characterized by vanishing vortex fugacity, and finite conductivities along both spatial directions. These two describe the quasi-localized phase and (critical) metal phase, respectively. The paper shows a direct transition between these two phases, supporting the universal emergence of the quasi-localized phase next to the (critical) metal phase in the 2D chiral unitary class.

An order-disorder transition of the U(1) NLSM in general D dimension is also induced by the spatial proliferation of vortex excitations [1, 2, 5–9, 11, 30, 46, 47]. Such vortex excitation takes a form of a closed loop of a vortex line in $D = 3$, and a closed surface of a vortex sheet in $D = 4$. The Berry phase term along x_0 direction generally endows each of these vortex excitations with a complex phase factor. For $D = 3$ and 4, the phase is proportional to an area inside the vortex loop projected on the x_1 - x_2 plane, and a volume inside the vortex surface projected on the x_1 - x_2 - x_3 space, respectively [31]. Such a complex phase factor induces destructive quantum interference among vortex excitations with finite projections in a space complementary to the x_0 axis. Meanwhile,

vortex excitations with no projection in the complementary subspace are free from the destructive interference effect, dominating the partition function near the transition point. As in $D = 2$, the proliferation of such polarized vortex excitations may result in the emergence of a quasi-disorder phase with a divergent correlation length along the x_0 direction, and finite correlation length along the others.

In order to establish a theory of such quasi-disorder phases in $D = 3$, this paper aims to develop a renormalization group (RG) theory of the $D = 3$ U(1) NLSM with the 1D Berry phase. We first introduce a model of the vortex loops whose segments interact with each other through the $1/|r|$ Coulomb interaction [1, 2, 7, 46, 48]. We derive RG equations among a vortex fugacity term, Berry phase term, and Coulomb interaction potential. In the presence of the Berry phase term, the isotropic Coulomb interaction $\mathcal{F}_1(r) = 1/|r|$ between two spatial points x and y with $r = x - y$ induces two other types of anisotropic interactions. Their interaction potentials are given by following 3 by 3 matrices;

$$\begin{aligned} \mathcal{F}_2(r) &= \frac{1}{|r|} \begin{pmatrix} 1 & & \\ & 1 & \\ & & -2 \end{pmatrix}, \\ \mathcal{G}(r) &= - \begin{pmatrix} 1 & & \\ & 1 & \\ & & -2 \end{pmatrix} \left(\frac{1}{|r|} - \frac{rr^T}{|r|^3} \right) \begin{pmatrix} 1 & & \\ & 1 & \\ & & -2 \end{pmatrix}, \end{aligned} \quad (2)$$

where two vortex segments, dx and dy , interact via $dx \cdot \mathcal{F}_2(r) \cdot dy$ and $dx \cdot \mathcal{G}(r) \cdot dy$, respectively. Here dx and dy are tangential vectors of vortex loops at x and y , respectively. A short-distance part of the $\mathcal{F}_2(r)$ interaction favors straight vortex lines polarized along the x_0 axis. $\mathcal{G}(r)$ takes a form of a dipolar interaction, which favors vortex loops curving within the x_1 - x_0 or x_2 - x_0 planes over vortex loops curving within the x_1 - x_2 plane. Upon renormalization, $\mathcal{F}_1(r)$, $\mathcal{F}_2(r)$ and $\mathcal{G}(r)$ further induce a spatial anisotropy between r_0 and $r_\perp = (r_1, r_2)$ with $r = (r_1, r_2, r_0)$. where the RG equations take functional forms of the three types of generic potentials of r_0 and $|r_\perp|$. By analyzing the functional RG equations approximately, we show that a characteristic length scale along the topological direction with the 1D Berry phase becomes anomalously large near a boundary of the ordered and disorder phases.

The paper is organized as follows. The next section introduces a 3D vortex loop model, where loop segments interact via the $1/|r|$ Coulomb interaction. We first develop a perturbative RG theory of the vortex loop model [section III], and study the loop model with the Berry phase term by the RG theory [section IV]. Firstly, we argue that the proliferation of the polarized vortex loops helps to develop the spatially anisotropic coherence of the U(1) order parameter [Section IVA]. Later, we derive the functional RG equations of the loop model with the Berry phase term [section IVB, C, D, and E], and analyze

the RG equations with approximations [section IVF, and G]. In section IVG, numerical solutions of the RG equation show that the characteristic vortex-loop size is divergent along the topological (x_0) direction near the transition point, while the vortex-loop size within the other directions remains finite. In terms of a duality mapping to the 3D type-II superconductors under the magnetic field, we also argue that a global phase diagram of the U(1) sigma model with the 1D Berry phase term must have the intermediate quasi-disorder phase between ordered and disorder phases [section V]. Appendices cover other topics useful in understanding the main text. In Appendix A, we discuss a linear confining potential between two end points of an open vortex line, and a form of associated dipole-dipole interaction. Appendix B and C provide supplemental details for the RG equations and analyses in Section IV.

II. FROM U(1) MODELS TO COULOMB LOOP GAS MODELS

Let us consider a partition function of Eq. (1) in a $L_1 \times L_2 \times L_0$ system with a periodic boundary condition. The phase variable $\theta(x)$ modulo 2π respects the Born-von Karman boundary condition, $\theta(x) = \theta(x + L_a) + 2\pi\mathbf{Z}$. Since Eq. (1) takes a quadratic action of its gradient vector, a spin-wave fluctuation around a uniform configuration $\theta(x) = \theta_0$ comprises only an action of a free theory; the spin-wave fluctuation on its own cannot drive an order-disorder transition. Thereby, topological excitations play a primary role in the phase transition of the U(1) NLSM. The U(1) phase has a 2D configuration with a pair of vortex and antivortex. In the 3D system, the vortex excitation forms a closed line – vortex loop –. A line integral of the gradient vector around the vortex line is quantized to 2π , $2\pi = \oint \nabla\theta \cdot d\mathbf{l} = \int \nabla \times \nabla\theta \cdot d\mathbf{n}$, relating a rotation of the gradient vector with a configuration of a vortex loop;

$$\begin{aligned} \nabla \times \nabla\theta(x) &= 2\pi \sum_{j=1}^n \int_{\Gamma_j} d\mathbf{x}^j \delta(x - x^j) \\ &= 2\pi \sum_{j=1}^n \int_0^{l_j} d\lambda \frac{d\mathbf{x}^j}{d\lambda} \delta(x - x^j(\lambda)). \end{aligned} \quad (3)$$

In Eq. (3), we consider a general case with n closed vortex loops Γ_j ($j = 1, \dots, n$). A spatial coordinate of the j -th vortex loop is given by a vector field $x^j \equiv (x_1^j, x_2^j, x_0^j)$. $\delta(x - x^j)$ is a delta function in 3D; $\delta(x - x^j) \equiv \delta(x_1 - x_1^j)\delta(x_2 - x_2^j)\delta(x_0 - x_0^j)$. $d\mathbf{x}^j$ is a tangential vector of the j -th vortex loop at x^j . The right-hand side is a parametric representation of Eq. (3) with a 1D length-scale parameter λ . l_j is a length of the j -th vortex loop, $d\mathbf{x}^j/d\lambda$ is the normalized tangential vector. Since all the vortex lines form closed loops, $x^j(0) = x^j(l_j)$ for $j = 1, \dots, n$.

The 1D Berry phase term confers a complex phase factor upon each of these vortex loops, and the phase for each vortex loop is proportional to a projected area of the loop onto the x_1 - x_2 plane [31],

$$S_1 \equiv i\chi \int d^3x \nabla_0\theta(x) = 2\pi i\chi \sum_{j=1}^n S_{12}^j. \quad (4)$$

S_{12}^j denotes the 2D projected area of the j -th loop. Here all the vortex loops are considered to be generated from the vacuum; when we contract the closed loops back into points by reducing their projected areas, $\theta(x)$ gets back to the uniform configuration. The sign of S_{12}^j is determined by a sign of the vorticity of the vortex loop. To see Eq. (4) with the sign, one can start with a vortex loop Γ and its projected area S . Choose the vorticity of the vortex loop to be anticlockwise when the projected area S on the x_1 - x_2 plane is seen from the $x_0 > 0$ side. Then, the 1D line integral of the gradient vector along the x_0 axis takes 2π and 0, when (x_1, x_2) is inside and outside the projected area S , respectively;

$$\int_0^{L_0} \nabla_0\theta(x_1, x_2, x_0) dx_0 = \begin{cases} 2\pi & \text{if } (x_1, x_2) \in S \\ 0 & \text{if } (x_1, x_2) \notin S. \end{cases} \quad (5)$$

As the winding number of the 1D Berry phase is additive with respect to an addition of the vortex loops, Eq. (5) readily gives Eq. (4) for the general n vortex-loops case.

A vortex-loop segment interacts with others via the $1/|r|$ Coulomb interaction [1, 2, 5]. To introduce the interaction, one can decompose the gradient vector into longitudinal u_L and transverse components u_T ; $\nabla\theta = u_L + u_T$, $\nabla \times u_L = 0$, and $\nabla \cdot u_T = 0$. This also decomposes the gradient term into longitudinal and transverse parts. Here the longitudinal part will be omitted, since it is only associated with the spin-wave fluctuation part Z_{sw} of the partition function [see Eq. (10)];

$$\begin{aligned} S_0 &\equiv \frac{1}{2T} \int \nabla\theta \cdot \nabla\theta d^3x = \frac{1}{2T} \int u_T^2 d^3x + \frac{1}{2T} \int u_L^2 d^3x \\ &= \frac{T}{2} \int H^2 d^3x + i \int H \cdot u_T d^3x + \dots \\ &= \frac{T}{2} \int (\nabla \times A)^2 d^3x - 2\pi i \int A(x) \cdot v(x) d^3x + \dots \end{aligned} \quad (6)$$

In the second line, the transverse part is decoupled in terms of a Stratonovich-Hubbard (SH) field H . The SH field thus introduced is a divergence-free vector field. Thus, a magnetic vector potential A can be further defined from the SH field, $H = \nabla \times A$. The vector potential here is divergence-free, as its longitudinal part would have nothing to do with the SH field. As all the vortex loops considered here are generated from the vacuum, trivial boundary conditions can be imposed on the vector potential, e.g. $A(x) = 0$ at the boundary of the system. Thereby, in the second term at the last line, we

can drop a surface term after a partial integral. From eq. (3), a vector $v(x) \equiv \frac{1}{2\pi} \nabla \times u_T$ is given by a sum of

$$v(x) = \sum_j \int_{\Gamma_j} dx^j \delta(x - x^j). \quad (7)$$

We henceforth call $v(x)$ as vortex vector.

The Coulomb interaction between the flux lines is obtained by the Gaussian integration over the vector potential. Completing the square in the momentum space yields:

$$S_0 = \int_{k \neq 0} \frac{dk^3}{(2\pi)^3} \left\{ \frac{Tk^2}{2} \left(A(k) - \frac{2\pi i}{Tk^2} v(k) \right)^T \left(1 - \frac{kk^T}{k^2} \right) \left(A(-k) - \frac{2\pi i}{Tk^2} v(-k) \right) + \frac{4\pi^2}{2Tk^2} v^T(k) \left(1 - \frac{kk^T}{k^2} \right) v(-k) \right\}. \quad (8)$$

As all the vortex loops considered here are closed loops, the vortex vector is also divergence free, $\nabla \cdot v(x) = 0$, and the integral over A gives the $1/|r|$ Coulomb interaction between the flux lines [1],

$$S_0 = \frac{\pi}{2T} \int d^3x \int d^3y \frac{v(x) \cdot v(y)}{|x - y|} = \frac{\pi}{2T} \sum_{i,j=1}^n \oint_{\Gamma_i} \oint_{\Gamma_j} \frac{dx^i \cdot dy^j}{|x^i - y^j|}. \quad (9)$$

In summary, the 3D U(1) NLSM can be described by a vortex-loop model, Eqs. (4,9);

$$Z = Z_{\text{sw}} Z_{\text{v}}, \quad Z_{\text{sw}} = \int du_L(x) \exp \left[-\frac{1}{2T} \int u_L^2 d^3x \right], \quad (10)$$

$$Z_{\text{v}} = 1 + \sum_{n=1}^{\infty} \frac{1}{n!} \prod_{j=1}^n \left(\int_a^{\infty} \left(\frac{dl_j}{a_0} \right) t^{l_j} \int \left(\frac{d^3R_j}{a_0^3} \right) \int D\Omega_j(\lambda) \right) \exp \left[-\frac{\pi}{2T} \sum_{i,j=1}^n \oint_{\Gamma_i} \oint_{\Gamma_j} \frac{dx^i \cdot dy^j}{|x^i - y^j|} - 2\pi i \chi \sum_{i=1}^n S_{12}^i \right]. \quad (11)$$

Here Z_{sw} and Z_{v} denote the longitudinal (spin-wave) part and transverse (vortex excitations) part of the partition function, respectively. Since the order-disorder transition in the U(1) NLSM is primarily driven by the proliferation of the vortex loops, this paper studies only Z_{v} .

In Z_{v} , we introduced a fugacity parameter “ t ” of vortex loop segment per the unit length; a chemical potential of the loop segment with the unit length is given by $\ln t$. We also introduced an ultraviolet (UV) cutoff “ a ” for an integral over the vortex-loop length l_j . The UV cutoff is on the order of a lattice constant a_0 of an underlying lattice model. R_j stands for a center-of-mass coordinate of the j -th loop. The integrals over the loop length l_j and over the center-of-mass coordinate R_j have the dimensions of length and volume, respectively. To make the partition function Z_{v} to be dimensionless, we divided them by the lattice constant a_0 , and by a unit volume a_0^3 , respectively. For simplicity of the notation, we omit these normalizations, $dl_j/a_0 \rightarrow dl_j$, $d^3R_j/a_0^3 \rightarrow d^3R_j$, while they will be recovered in the end of RG calculations.

$\Omega^j(\lambda) \equiv dx^j(\lambda)/d\lambda$ is a normalized tangential vector along the j -th loop at a segment λ . A path integral over the normalized tangential vectors for $\lambda \in [0, l_j]$ takes a summation over all possible shapes of the closed loop

with a fixed length l_j ;

$$\int D\Omega^j(\lambda) \equiv \lim_{\varepsilon \rightarrow 0} \prod_{M=1}^{l_j/\varepsilon} \left(\int_{\int_0^{l_j} \Omega^j(\lambda) d\lambda = 0} d\Omega^j(\lambda = M\varepsilon) \right). \quad (12)$$

As $\Omega^j(\lambda)$ is a unit vector, the path integral over $\Omega^j(\lambda)$ is independent from the length scale. A factor $1/n!$ in Eq. (11) is a symmetric factor that sets off double counting of an identical configuration of the n vortex loops.

The $1/|r|$ Coulomb interaction between the vortex-loop segments also needs a UV cutoff. We use the lattice constant a_0 as the UV cutoff for the Coulomb interaction length;

$$\oint_{\Gamma_i} \oint_{\Gamma_j} \frac{dx^i \cdot dy^j}{|x^i - y^j|} \equiv \oint \oint_{|x^i - y^j| > a_0} \frac{dx^i \cdot dy^j}{|x^i - y^j|}. \quad (13)$$

A ratio between “ a ” and “ a_0 ” is generally model-dependent. In section III, we will explain our choice of the UV model in this paper.

In the next section, we first develop a renormalization group (RG) study of Z_{v} without the Berry phase ($\chi = 0$). We derive coupled RG equations between the

fugacity parameter t and stiffness parameter $1/T$. The RG equations have a strong coupling fixed point with divergent fugacity (disorder phase), a weak coupling fixed point with vanishing fugacity (order phase), and a saddle-point fixed point between these two. A scaling analysis around the saddle-point fixed point gives us an estimate of a critical exponent of an order-disorder transition of the 3D U(1) NLSM without the Berry phase term.

III. RG ANALYSIS OF A 3D COULOMB LOOP GAS MODEL

A renormalization comprises an integration over short-distance degrees of freedom (DOF) and a rescaling of the length scale [5, 47, 49, 50]. The integration is carried out perturbatively in $1/T$, giving 1-loop renormalization to the two coupling constants, T and t . The integration also changes the UV cutoffs “ a ” and “ a_0 ” into “ ab ” and “ a_0b ”, respectively, where an infinitesimally small positive $\ln b$ plays the role of an RG rescaling factor. The subsequent

length rescaling puts the UV cutoffs back to the original values.

$$\begin{aligned} x^i &\rightarrow x^{i'} = x^i b^{-1}, \quad y^j \rightarrow y^{j'} = y^j b^{-1}, \quad l_j \rightarrow l'_j = l_j b^{-1}, \\ R_j &\rightarrow R'_j = R_j b^{-1}, \quad \lambda \rightarrow \lambda' = \lambda b^{-1}. \end{aligned} \quad (14)$$

The inverse temperature and the chemical potential of the vortex loop segment have their tree-level scaling dimensions to be 1 ,

$$\frac{1}{T} \rightarrow \frac{1}{T'} = \frac{1}{T} b, \quad \ln t \rightarrow \ln t' = \ln t b, \quad (15)$$

[[$1/T$] = 1, [$\ln t$] = 1].

To integrate over the short-distance DOF [5, 49], we decompose an integral of the loop length l into an integral over its short-length region ($a < l < ab$) and the integral over its long-length region ($ab < l$); $\int_a^\infty dl = \int_a^{ab} dl + \int_{ab}^\infty dl$. Substitute it into Eq. (11), and keep up to the first order in small $\ln b$;

$$\begin{aligned} Z_v = &1 + \left(\int_a^{ab} dt t^l \int d^3 R \int D\Omega(\lambda) \right) e^{-s_0(\Gamma, \Gamma)} + \sum_{n=1}^{\infty} \frac{1}{n!} \prod_{j=1}^n \left(\int_{ab}^{\infty} dl_j t^{l_j} \int d^3 R_j \int D\Omega_j(\lambda) \right) e^{-\sum_{i,j=1}^n s_0(\Gamma_i, \Gamma_j)} \\ &+ \left(\int_a^{ab} dt t^l \int d^3 R \int D\Omega(\lambda) \right) \sum_{n=1}^{\infty} \frac{1}{n!} \prod_{j=1}^n \left(\int_{ab}^{\infty} dl_j t^{l_j} \int d^3 R_j \int D\Omega_j(\lambda) \right) e^{-s_0(\Gamma, \Gamma) - 2\sum_{j=1}^n s_0(\Gamma, \Gamma_j) - \sum_{i,j=1}^n s_0(\Gamma_i, \Gamma_j)} \end{aligned} \quad (16)$$

Here Γ is the shortest closed loop with its length being in $a < l < ab$. $\int d^3 R \int D\Omega(\lambda)$ stands for a configurational integral of the shortest loop; R and $\Omega(\lambda)$ are a center-of-mass coordinate and the tangential vectors of the shortest loop. $s_0(\Gamma_i, \Gamma_j)$ is the Coulomb interaction between the i -th and j -th loops;

$$s_0(\Gamma_i, \Gamma_j) = \frac{\pi}{2T} \oint_{\Gamma_i} \oint_{\Gamma_j} \frac{dx^i \cdot dy^j}{|x^i - y^j|}. \quad (17)$$

To carry out the configurational integral over the shortest loop, we expand the Coulomb interaction $s_0(\Gamma, \Gamma_j)$ between the shortest loop and the other loops,

$$\begin{aligned} Z_v = &1 + \left(\int_a^{ab} dt t^l \int d^3 R \int D\Omega(\lambda) \right) e^{-s_0(\Gamma, \Gamma)} + \sum_{n=1}^{\infty} \frac{1}{n!} \prod_{j=1}^n \left(\int_{ab}^{\infty} dl_j t^{l_j} \int d^3 R_j \int D\Omega_j(\lambda) \right) e^{-\sum_{i,j=1}^n s_0(\Gamma_i, \Gamma_j)} \\ &+ \sum_{n=1}^{\infty} \frac{1}{n!} \prod_{j=1}^n \left(\int_{ab}^{\infty} dl_j t^{l_j} \int d^3 R_j \int D\Omega_j(\lambda) \right) e^{-\sum_{i,j=1}^n s_0(\Gamma_i, \Gamma_j)} \\ &\times \left(\int_a^{ab} dt t^l \int d^3 R \int D\Omega(\lambda) \right) e^{-s_0(\Gamma, \Gamma)} \left\{ 1 - \left(\sum_{j=1}^n 2s_0(\Gamma, \Gamma_j) \right) + \frac{1}{2} \left(\sum_{j=1}^n 2s_0(\Gamma, \Gamma_j) \right)^2 + \dots \right\} \end{aligned} \quad (18)$$

The expansion is perturbative in $1/T$, and it is justified a posteriori by an observation that an inverse temperature around the saddle fixed point is small. Note that the temperature T in this paper has a dimension of length,

so that the temperature shall be compared to the UV cutoff length a_0 in the observation.

After the configurational integral of the shortest loop, the fourth term in Eq. (18) gives a renormalization to the

temperature in the third term. More specifically, the first order in $s_0(\Gamma, \Gamma_j)$ vanishes after the configurational sum, while the second-order in $s_0(\Gamma, \Gamma_j)$ induces a renormalization to the Coulomb interaction among the rest of the other loops. The renormalization is nothing but a screening effect caused by the shortest loop. The second term in Eq. (18) is extensive because of its R integral, while it is also on the order of $\ln b$. Thus, the second term can be included as an inhomogeneous part of a free-energy renormalization. Since we are primarily interested in the RG equations among the coupling constants, we do not delve ourselves into the free-energy renormalization in this paper.

The Coulomb interaction $s_0(\Gamma_i, \Gamma_j)$ in the third term needs to be also decomposed into short-distance part and long-distance part [5, 49];

$$\begin{aligned} & \oint_{\Gamma_i} \oint_{\Gamma_j} \frac{|x^i - y^j| > a_0}{|x^i - y^j|} dx^i \cdot dy^j \\ &= \left(\oint_{\Gamma_i} \oint_{\Gamma_j} \frac{a_0 b > |x^i - y^j| > a_0}{|x^i - y^j|} + \oint_{\Gamma_i} \oint_{\Gamma_j} \frac{|x^i - y^j| > a_0 b}{|x^i - y^j|} \right) dx^i \cdot dy^j \end{aligned} \quad (19)$$

The short-distance part of the Coulomb interaction within a same loop Γ_i gives a renormalization to the fugacity for the loop.

$$\oint_{\Gamma_i} \oint_{\Gamma_i} \frac{a_0 b > |x^i - y^i| > a_0}{|x^i - y^i|} dx^i \cdot dy^i = 2 \ln b l_i + \dots \quad (20)$$

Here “...” in the right hand side stands for renormalization to other physical parameters associated with a vortex loop. Such parameters include an elastic energy parameter u of the vortex loop. To see Eq. (20), one can use the parametric representation of the loop and expand the normalized tangential vectors in terms of the short-distance a_0 ;

$$\begin{aligned} & \oint_{\Gamma_i} \oint_{\Gamma_i} \frac{a_0 b > |x^i - y^i| > a_0}{|x^i - y^i|} dx^i \cdot dy^i \\ &= \int_0^{l_i} d\lambda \int_{b a_0 > |\lambda' - \lambda| > a_0} d\lambda' \frac{\Omega_i(\lambda) \cdot \Omega_i(\lambda')}{|\lambda - \lambda'|} \\ &= 2 \ln b l_i + \delta u \ln b \int_0^{l_i} d\lambda \left| \frac{\partial \Omega_i}{\partial \lambda} \right|^2 + \dots \end{aligned} \quad (21)$$

Here $\delta u = -\frac{1}{2} a_0^2$ is the renormalization to the elastic energy parameter u . Since the elastic energy parameter u has a negative tree-level scaling dimension ($[u] = -1$), we will omit this effect in this paper, and consider only the renormalization to the vortex fugacity parameter, i.e. $2 \ln b l_i$. The short-distance part of the Coulomb interaction between different loops ($i \neq j$) may induce renormalization to physical parameters of a vortex loop when the two loops merge at some vortex segments. Unlike the fugacity renormalization, however, such merging

events happen only occasionally upon the renormalization. Thus, we ignore by hand the short-distance part of the Coulomb interaction between different loops.

To calculate the renormalization to the temperature, we need to specify the shortest loop in detail. To this end, let us be inspired by a lattice-regularized model on a cubic lattice. A lattice point of the cubic lattice accommodates the U(1) phase variable $\theta(x)$, and its lattice constant a_0 is the UV cutoff for the Coulomb interaction length in Eq. (13). A dual lattice is also a cubic lattice. Nearest neighboring sites of the dual lattice are connected by the vortex vector $v(x)$, and the square plaquette of the dual lattice forms the shortest vortex loop. As a counterpart of such square-plaquette loop, we choose a symmetric circle with its diameter a_0 as the shortest loop in the continuum theory. The choice of the shortest loop sets the UV cutoff a for the loop length in Eq. (11); $a = a_0 \pi$. Here, the shortest loops with other shapes, e.g. elliptical circle, non-coplanar closed loop, are not considered as physical loops. For example, an ellipse with its circumference $a_0 \pi$ has its diameter along its minor axis to be shorter than a_0 . We do not consider such elliptical circles as physical because two flux lines with the opposite vorticity cannot be closer than the lattice constant a_0 on the dual lattice.

The shortest loop thus introduced is always coplanar, so that a unit vector Ω normal to the plane, and a center of the circle entirely parameterize the configuration of the loop. The configuration sum of the shortest loop comprises of an integral over the center coordinate R over a whole volume V , and a 2D integral with respect to Ω over a unit sphere S_2 ,

$$\int_a^{ab} dl \int d^3 R \int D\Omega(\lambda) = a \ln b \int_V d^3 R \int_{S_2} d^2 \Omega. \quad (22)$$

The spatial coordinate x and tangential vector dx of the loop segment in the short loop can be parameterized by an angle $\alpha \in [0, 2\pi)$,

$$x = R + \frac{a_0}{2} n(\alpha), \quad dx = \frac{a_0}{2} \frac{dn}{d\alpha} \equiv \frac{a_0}{2} m(\alpha), \quad (23)$$

with $n(\alpha) = \cos \alpha (-e_2) + \sin \alpha e_1$, and $m(\alpha) = \cos \alpha e_1 + \sin \alpha e_2$. Here e_1 and e_2 are orthonormal vectors on the coplanar plane, and e_1, e_2 and Ω form an orthonormal basis frame with $e_1 \times e_2 = \Omega$.

To evaluate the screening effect by the short vortex loop, note first that the UV cutoff a_0 is much smaller than the temperature, so that we could also expand $s_0(\Gamma, \Gamma_j)$

in powers of the diameter of the circular loop Γ ;

$$\begin{aligned}
2s_0(\Gamma, \Gamma_j) &= \frac{\pi}{T} \int_{\Gamma} \int_{\Gamma_j} \frac{dx \cdot dy^j}{|x - y^j|} \\
&= \frac{\pi}{T} \frac{a_0}{2} \int_0^\pi d\alpha \int_{\Gamma_j} \frac{m(\alpha) \cdot dy^j}{|R + \frac{a_0}{2} n(\alpha) - y^j|} \\
&\quad - \frac{\pi}{T} \frac{a_0}{2} \int_0^\pi d\alpha \int_{\Gamma_j} \frac{m(\alpha) \cdot dy^j}{|R - \frac{a_0}{2} n(\alpha) - y^j|} \\
&= \frac{\pi a_0^2}{2T} \int_{\Gamma_j} dy_\nu^j \int_0^\pi d\alpha m_\nu(\alpha) n_\mu(\alpha) \nabla_{R_\mu} \left(\frac{1}{|R - y^j|} \right) + \dots \\
&= \frac{\pi^2 a_0^2}{4T} \int_{\Gamma_j} dy_\nu^j \Omega_\lambda \epsilon_{\lambda\mu\nu} \nabla_{R_\mu} \left(\frac{1}{|R - y^j|} \right) + \dots \quad (24)
\end{aligned}$$

Upon a substitution of this into Eq. (18), the integral over Ω makes the first order in $s_0(\Gamma, \Gamma_j)$ vanish in Eq. (18), while the second order term in $s_0(\Gamma, \Gamma_j)$ yields the effective Coulomb interaction among the other loops,

$$\begin{aligned}
&\int_V d^3R \int_{S_2} d^2\Omega \left\{ 1 + \frac{1}{2} \left(\sum_{j=1}^n 2s_0(\Gamma, \Gamma_j) \right)^2 + \dots \right\} \\
&= 4\pi V + \frac{2\pi}{3} \left(\frac{\pi^2 a_0^2}{4T} \right)^2 \sum_{i,j=1}^n \int d^3R \\
&\left\{ \oint_{\Gamma_i} dx_\lambda^i \oint_{\Gamma_j} dy_\lambda^j \nabla_{R_\mu} \left(\frac{1}{|R - x^i|} \right) \nabla_{R_\mu} \left(\frac{1}{|R - y^j|} \right) - \right. \\
&\left. \oint_{\Gamma_i} dx_\lambda^i \oint_{\Gamma_j} dy_\mu^j \nabla_{R_\mu} \left(\frac{1}{|R - x^i|} \right) \nabla_{R_\lambda} \left(\frac{1}{|R - y^j|} \right) \right\} + \dots, \\
&= 4\pi V + \frac{2\pi^2}{3} \left(\frac{\pi^2 a_0^2}{2T} \right)^2 \sum_{i,j=1}^n \oint_{\Gamma_i} \oint_{\Gamma_j} \frac{dx^i \cdot dy^j}{|x^i - y^j|} + \dots \quad (25)
\end{aligned}$$

Here we took an integration by parts with respect to R_μ in the second line, and used $\nabla_R^2(1/|R-x|) = -4\pi\delta(R-x)$ for the first term. We also note that the loop is closed so that $\oint_{\Gamma_j} dy_\mu^j \nabla_{R_\mu} f(R-y^j) = -\oint_{\Gamma_j} dy_\mu^j \nabla_{y_\mu^j} f(R-y^j) = 0$ for the second term in the second line.

A substitution of Eqs. (20,25) into Eq. (18) yields an effective action only for the longer vortex loops up to the first order in $\ln b$,

$$\begin{aligned}
Z_V &= e^{4\pi V a t^a \ln b} \left\{ 1 + \sum_{n=1}^{\infty} \frac{1}{n!} \right. \\
&\left. \prod_{j=1}^n \left(\int_{ab}^{\infty} dl_j (\bar{t})^{l_j} \int d^3R_j \int D\Omega_j(\lambda) \right) e^{-\sum_{i,j=1}^n \bar{s}_0(\Gamma_i, \Gamma_j)} \right\}, \quad (26)
\end{aligned}$$

where

$$\bar{s}_0(\Gamma_i, \Gamma_j) = \frac{\pi}{2T} \oint_{\Gamma_i} \oint_{\Gamma_j}^{|x_i - y_j| > a_0 b} \frac{dx^i \cdot dy^j}{|x^i - y^j|}, \quad (27)$$

with

$$\ln \bar{t} = \ln t - \frac{\pi}{T} \ln b, \quad (28)$$

$$\frac{\pi}{2\bar{T}} = \frac{\pi}{2T} - at^a \frac{2\pi^2}{3} \left(\frac{\pi^2 a_0^2}{2T} \right)^2 \ln b, \quad (29)$$

and $a = a_0\pi$. Note that $s_0(\Gamma, \Gamma) \propto \ln b$ is omitted in Eq. (26) because its contribution appears in the partition function with the higher power in $\ln b$. Combining these renormalization with the length rescaling in Eq. (14), we finally obtain

$$\ln t' = \ln \bar{t} b = \ln t + \ln t \ln b - \frac{\pi}{T} \ln b, \quad (30)$$

$$\begin{aligned}
\frac{\pi}{2T'} &= \frac{\pi}{2\bar{T}} b \\
&= \frac{\pi}{2T} + \frac{\pi}{2T} \ln b - at^a \frac{2\pi^2}{3} \left(\frac{\pi^2 a_0^2}{2T} \right)^2 \ln b. \quad (31)
\end{aligned}$$

These two yield coupled RG equations between T and $\ln t$;

$$\frac{d \ln t}{d \ln b} = \ln t - \frac{\pi}{T}, \quad (32)$$

$$\frac{d}{d \ln b} \left(\frac{\pi}{2T} \right) = \frac{\pi}{2T} - a_0 e^{a_0\pi \ln t} \frac{2\pi^3}{3} \left(\frac{\pi^2 a_0^2}{2T} \right)^2. \quad (33)$$

Before proceeding to a fixed-point analysis of the RG equation, let us note that the length rescaling in $\int dl_j \int d^3R_j$ induces an additional factor of b^4 for each vortex loop. This factor can be included into a renormalization of another type of vortex fugacity parameter v that does not depend on the loop length; $t^{l_j} \rightarrow t^{l_j} v$, together with $v' = b^4 v$ [5]. The scaling equation of v gives

$$\frac{d \ln v}{d \ln b} = 4. \quad (34)$$

A comparison between Eqs. (32,34) suggests that t decreases/increases exponentially in the RG scale factor $\ln b$, while v increases only in the power of b . Such t always dominates over v , when t decreases as well as increases. Thus, the order and disorder phases can be determined only by divergent and vanishing t , respectively, and we ignore the scaling equation of v henceforth. Eqs. (32,33,34) are consistent with a set of RG equations that Williams and Shenoy derived previously in studies of the superfluid λ transition [5, 47, 51–54]. The RG equations were also applied to the studies of cosmic strings in the early universe [55, 56] and high-Tc superconductors [12–14, 41, 53]. For completeness, we will give a fixed-point analysis of Eqs. (32,33) below.

To analyze fixed points of Eqs. (32,33), we first normalize T and $\ln t$ by the UV cutoff length scale a_0 . Besides, we will also recover the normalization factor of the integrals over l_j and R_j for each loop [see a text between Eqs. (11,12)]. This gives the dimensionless RG equations for $x \equiv a_0 \ln t$ and $y \equiv \frac{\pi a_0}{2T}$ as follows,

$$\frac{dx}{d \ln b} = x - 2y, \quad \frac{dy}{d \ln b} = y - \frac{2\pi^5}{3} e^{\pi x} y^2. \quad (35)$$

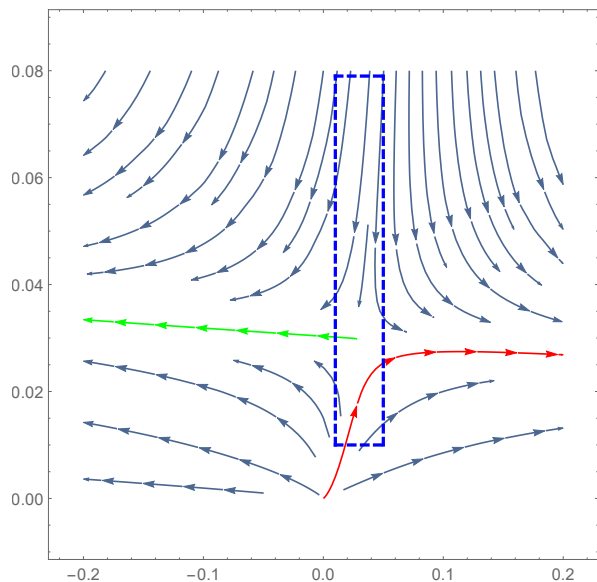


FIG. 1. An RG flow diagram of 3D Coulomb loop gas model without the 1D Berry phase term. It is obtained from Eqs. (32,33), where the horizontal and vertical axes are $\pi x = \pi a_0 \ln t$, and $2\pi y = \pi^2 a_0/T$ respectively. The green flow goes to a low- T fixed point at $(t, T) = (0, 0)$, and red flow goes to a high- T fixed point at $(t, T) = (\infty, \infty)$. A saddle fixed point at $(\pi x, 2\pi y) = 0.0299\dots(1, 1)$ determines the criticality of the order-disorder transition.

The RG equations have a high- T fixed point with divergent fugacity parameter t at $(x, y) = (\infty, 0)$, a low- T fixed point with vanishing fugacity parameter at $(x, y) = (-\infty, \infty)$, and a saddle fixed point at $(x, y) = y_0(2, 1)$ with $y_0 = 0.00485\dots$. The fixed point with divergent fugacity t and divergent T characterizes the disorder phase of the NLSM, while the fixed point with vanishing fugacity t and vanishing T is for the order phase. A linearization around the saddle fixed point

$$\frac{d}{d \ln b} \begin{pmatrix} x \\ y \end{pmatrix} = \begin{pmatrix} 1 & -2 \\ -y_0\pi & -1 \end{pmatrix} \begin{pmatrix} x \\ y \end{pmatrix} \quad (36)$$

gives a scaling dimension y_t of the relevant scaling variable around the saddle fixed point to be $y_t \simeq 1 + y_0\pi = 1.0153\dots$ and critical exponent $\nu \equiv 1/y_t$ for the order-disorder transition to be $\nu = 0.984\dots$. Note that a small value of $y_0 \simeq 0.005$ at the saddle fixed point justifies a posteriori the perturbative expansion with respect to a_0/T in Eqs. (18).

The value of y at the saddle-point fixed point depends on a choice of the shortest loop, and in this respect, the perturbative RG analysis may not be “controlled”. To make the perturbative expansion in a_0/T to be truly controlled as in the Wilson-Fisher theory [57, 58], one can generalize the 3D model into a D -dimensional model with $1/|r|^{D-2}$ Coulomb interaction [51]. In the D -dimensional model, the vortex excitation takes a form of $(D-2)$ -dimensional hypersphere. The fugacity parameter $\ln t$ for the vortex hypersphere is introduced as a chemical

potential per unit volume in the $D-2$ dimension. The fugacity parameter $\ln t$ for the vortex supersphere is introduced as a chemical potential per unit volume in the $D-2$ dimension. $\ln t$ as well as the inverse temperature are normalized by a_0^{D-2} . Under the scaling of Eq. (14), the 1-loop RG equations for these normalized coupling constants, x and y , take the following forms of

$$\begin{aligned} \frac{dx}{d \ln b} &= (D-2)x - Ay, \\ \frac{dy}{d \ln b} &= (D-2)y - Be^{Cx}y^2. \end{aligned} \quad (37)$$

It is expected that A , B , and C are analytic functions of the spatial dimension D around $D=2$, and B and C are finite at $D=2$. Thus, by $D=2+\epsilon$, the value of y at the saddle fixed point is on the order of the small ϵ . We leave an ϵ -expansion analysis of the D -dim. model for future work.

IV. RG ANALYSIS OF A 3D COULOMB LOOP GAS WITH THE 1D BERRY PHASE TERM

In the previous section, we have developed a perturbative RG theory of the 3D Coulomb loop gas model. In this section, we use the perturbative RG theory to study the loop gas model with the 1D Berry phase term. According to the partition function Eq. (11), the 1D Berry phase factor for each vortex loop is proportional to an area within the loop projected onto the x_1 - x_2 plane. Such complex phase factor induces a destructive interference among the vortex loops with finite projections onto the x_1 - x_2 plane. Meanwhile, those loops that are confined in planes parallel to the x_0 -axis are free from the destructive interference, dominating the partition function near the order-disorder transition point. In the next subsection, we first discuss how the proliferation of such polarized vortex loops leads to an extremely spatially anisotropic correlation of the U(1) order parameter.

A. spatially anisotropic phase coherence induced by the interference effect

The proliferation of the vortex loops polarized along the x_0 axis renders a correlation of $e^{i\theta(x)}$ within the x_1 - x_2 plane to be strongly disordered, while leaving the correlation along the x_0 axis intact. To see this anisotropy, let us consider a relative U(1) phase between the two “test” points y and z ; $\theta(y, z) \equiv \theta(y) - \theta(z)$, and see how much an add-on phase $e^{i\delta\theta(y, z)}$ the relative phase $e^{i\theta(y, z)}$ acquires from an introduction of a polarized vortex loop. A vortex loop Γ induces a magnetic scalar potential $\theta_m(x)$; $\nabla \times \nabla\theta_m(x) = \oint_{\Gamma} dx' \delta(x-x')$, and the magnetic scalar potential changes the relative U(1) phase; $\theta(y, z) \rightarrow \theta(y, z) + \theta_m(y) - \theta_m(z)$. Such phase change is given by a line integral of a magnetic field

$B(x) = -\nabla\theta_m(x)$ along an arbitrary line connecting y and z ;

$$\delta\theta(y, z) = \int_y^z dx \cdot B(x). \quad (38)$$

$\delta\theta(y, z)$ is determined up to a multiple of 2π . Arbitrary multiple of 2π comes from a choice of the integral line, while $\exp[i\delta\theta(y, z)]$ is free from the choice of the integral line,

$$e^{i\delta\theta(y, z)} = \exp \left[i \int_y^z dx \cdot B(x) \right]. \quad (39)$$

The Biot-Savart law gives $B(x)$ as a "magnetic induction" generated by a "quantized electric current" along the loop [59];

$$B(x) = \frac{1}{2} \oint_{\Gamma} dx' \times \nabla \left(\frac{1}{|x - x'|} \right). \quad (40)$$

In the perpendicular geometry [$y - z \perp$ the x_0 axis], the add-on phase $e^{i\delta\theta(y, z)}$ always rotates 360 degrees around the origin in the complex plane when the polarized vortex loop extends from a shorter loop to a larger loop. In the parallel geometry [$y - z \parallel$ the x_0 axis], however, it does not make the rotation around the origin. To see the phase winding in the perpendicular geometry, let us place the two test points y and z along the x_2 axis, $y_0 = z_0$, $y_1 = z_1$, and $y_2 > z_2$ [Fig. 2], and choose the x_2 axis as an integral line in Eqs. (38,39),

$$\delta\theta(y, z) = \int_{y_2}^{z_2} dx_2 B_2(y_0, y_1, x_2). \quad (41)$$

Consider that a small circular loop is introduced in a x_1 - x_0 plane between y and z , $y_2 < R_2 < z_2$, and its center-of-mass coordinate R is fixed far away from y and z , $(y_2 - z_2)^2 \ll (R_0 - y_0)^2 + (R_1 - y_1)^2$ [see Fig. 2]. The vorticity of the loop is counterclockwise when viewed from y .

When the circular loop extends from a smaller loop to a larger loop, the complex unit number $e^{i\delta\theta(y, z)}$ always makes one full counterclockwise rotation around the origin [Fig. 2]. For the smaller loop, the magnetic field around the test points is small; so is $\delta\theta(y, z)$ in Eq. (41); $\delta\theta(y, z) \simeq 0$. When the loop gets larger, some segment of the loop is nearing the test points, which increases the magnetic field $B(y_0, y_1, R_2)$ at (y_0, y_1, R_2) along the $-x_2$ direction. When the segment crosses (y_0, y_1, R_2) , the magnetic field $B(y_0, y_1, R_2)$ changes its direction from $-x_2$ direction into the $+x_2$ direction. Importantly, $\delta\theta(y, z)$ defined in eq. (41) takes values of $\pi - 0$ and $-\pi + 0$ before and after the segment crosses (y_0, y_1, R_2) . When the loop becomes even larger, the field strength at the test points decreases with the power of the distance between the segment and the test points. Thus, the unit complex number $e^{i\delta\theta(y, z)}$ makes a full counterclockwise rotation around the origin in the complex plane during the change of the loop size.

The argument so far does not depend on the detailed shapes of the vortex loop, as well as its center-of-mass coordinate R . It holds in other geometry with a finite angle between $y - z$ and the x_0 axis, as far as a loop segment crosses the line between y and z during the size change of the polarized loop. Namely, the winding of $e^{i\delta\theta(y, z)}$ around the unit circle depends only on how many times a vortex segment crosses the line between y and z . In a geometry with a finite angle between $y - z$ and the x_0 axis, there always exist polarized vortex loops, whose segment crosses the line between y and z during the change of the loop size. Due to the phase windings, the add-on phase $\langle e^{i\delta\theta(y, z)} \rangle$ averaged over different sizes of the polarized vortex loops with the same fugacity ($[\ln t = 0]$) always reduces to zero. On the other hand, in the parallel geometry [$y - z \parallel$ the x_0 axis], no coplanar vortex loop confined in planes parallel to the x_0 axis can cross the line between y and z during its size change. Thus, an add-on phase averaged over the polarized loops with different sizes remains finite. This suggests that the proliferation of the polarized loop only destroys the phase coherence within the x_1 - x_2 plane.

Ultimately, the anisotropic phase coherence near the order-disorder transition point helps an emergence of a quasi-disorder phase between ordered and disorder phases. In the quasi-disorder phase, the U(1) order parameter has a divergent correlation length along the x_0 direction, and a finite correlation length within the other directions. To aim at a theoretical description of such a quasi-disorder phase, we develop, in the remaining part of this section, the perturbative RG theory for the loop-gas model with the 1D Berry phase term.

B. Generic form of the 3D Coulomb interactions

In the presence of the Berry phase term, the Coulomb interaction potential acquires emergent anisotropies both in space and in vortex-vector space. A generic form of the emergent interaction potential is determined by symmetries of a bare action in Eqs. (4,9). Suppose that the interaction among vortex-loop segments is described by a two-body interaction potential between vortex vectors at x and at y ;

$$S_0[v(x)] \equiv \int d^3x \int d^3y v(x) \cdot H(x - y) \cdot v(y). \quad (42)$$

As the two vectors are commutable, a 3 by 3 matrix-formed potential $H(x - y)$ is symmetrized, $H(x - y) = H^T(y - x)$. The bare action in Eqs. (4,9) has an inversion symmetry, $v(x) \rightarrow -v(-x)$, as well as a continuous

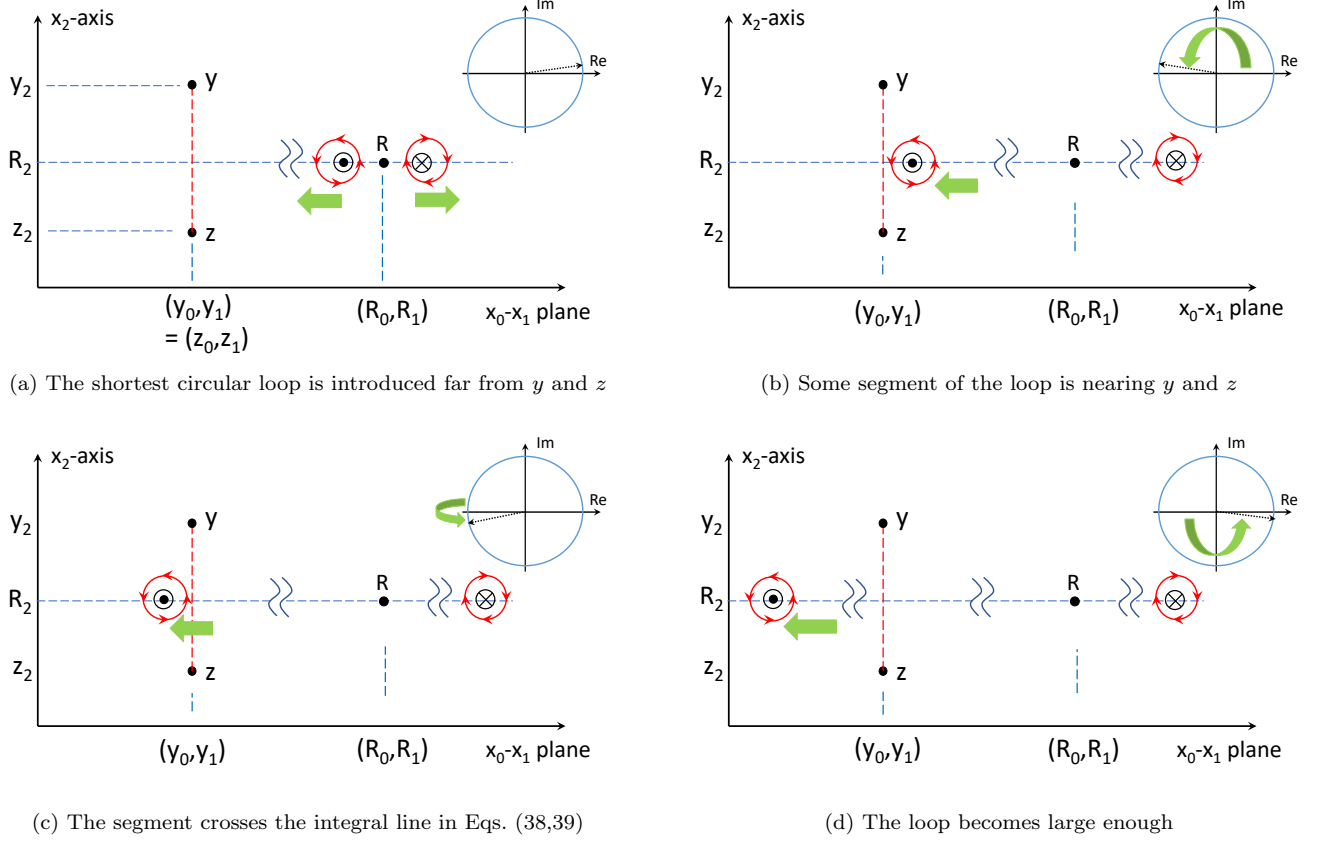


FIG. 2. Four schematic figures explain how $e^{i\delta\theta(y,z)}$ moves along the unit circle in the complex plane when a vortex loop extends from a shorter loop to a larger loop in the perpendicular geometry [$y - z \perp$ the x_0 axis]. Small figure in the upper right corner of each figure shows the motion of $e^{i\delta\theta(y,z)}$ along the unit circle. Here, $y - z$ is along the x_2 axis, and a circular and coplanar vortex loop is placed on a x_0 - x_1 plane between y and z . A cross section of the vortex loop is denoted by \odot and \otimes . Red lines with arrows denote a distribution of the magnetic field B around the vortex loop. The center-of-mass coordinate R of the loop is fixed far from the test points, y, z , while the diameter of the circular loop changes from a shorter length to a larger length. The integral line of Eqs. (38,39) is shown by a vertical dashed red line connecting y and z . (a) When the loop is small, so is the magnetic field near the test points; $e^{i\delta\theta(y,z)} \simeq 0$. (b) When the loop gets larger and some segment of the loop is approaching the test points, the magnetic field near the test points is along $-x_2$ direction, and $\delta\theta(y, z)$ in Eq. (38) increases from 0 to $\pi - 0$; $e^{i\delta\theta(y,z)}$ rotates from 0 to $-1 + i0$. (c) When the segment crosses (y_0, y_1, R_2) , the magnetic field in Eq. (38) changes its sign, and $\delta\theta(y, z)$ changes from π to $-\pi$; $e^{i\delta\theta(y,z)}$ moves from $-1 + i0$ to $-1 - i0$. (d) When the loop becomes large enough, the magnetic field near the test points becomes smaller again; $e^{i\delta\theta(y,z)}$ comes back to $+1$.

rotational symmetry around the x_0 axis,

$$v(x) \rightarrow \bar{v}(\bar{x}) \equiv \begin{pmatrix} \cos \varepsilon & \sin \varepsilon & \\ -\sin \varepsilon & \cos \varepsilon & \\ & & 1 \end{pmatrix} v(x),$$

$$\bar{x} \equiv \begin{pmatrix} \cos \varepsilon & \sin \varepsilon & \\ -\sin \varepsilon & \cos \varepsilon & \\ & & 1 \end{pmatrix} x. \quad (43)$$

So does the interaction potential; $H(x - y) = H(y - x) = H^T(y - x)$ and

$$H(x - y) = \begin{pmatrix} \cos \varepsilon & -\sin \varepsilon & \\ \sin \varepsilon & \cos \varepsilon & \\ & & 1 \end{pmatrix} H(\bar{x} - \bar{y}) \begin{pmatrix} \cos \varepsilon & \sin \varepsilon & \\ -\sin \varepsilon & \cos \varepsilon & \\ & & 1 \end{pmatrix}. \quad (44)$$

The interaction potential in this section is most conveniently analyzed in terms of its Fourier transform $H(q)$,

$$H(x - y) \equiv \int_{q \neq 0} \frac{d^3 q}{(2\pi)^3} H(q) e^{-iq(x-y)}, \quad (45)$$

with momentum $q \equiv (q_1, q_2, q_0)$. In the right hand side, we take a principal value around $q = 0$, because

$\int d^3x v(x) = 0$. The symmetries of $H(x-y)$ determine a form of 3 by 3 matrix $H(q)$ as,

$$H(q) = F_1(q) + F_2(q) \eta_2 + G_0(q) (b_1(q) + \eta_2) \hat{q} \hat{q}^T (b_1(q) + \eta_2), \quad (46)$$

with a traceless diagonal matrix η_2 ,

$$\eta_2 \equiv \begin{pmatrix} 1 & & \\ & 1 & \\ & & -2 \end{pmatrix}. \quad (47)$$

Here $\hat{q} \equiv q/|q|$ is a normalized q vector, and a trace of a symmetric matrix $\hat{q} \hat{q}^T$ is 1. F_1 , F_2 , G_0 and b_1 are scalar functions of $q_\perp \equiv (q_1, q_2)$ and q_0 . They are symmetric under the continuous rotation and inversion; $F_1(q) \equiv F_1(|q_\perp|, |q_0|)$, $F_2(q) \equiv F_2(|q_\perp|, |q_0|)$, $G_0(q) \equiv G_0(|q_\perp|, |q_0|)$, $b_1(q) \equiv b(|q_\perp|, |q_0|)$. In the partition function with closed vortex loops, $b_1(q)$ terms in $H(q)$ do not contribute to \mathcal{S}_0 , because they all appear in

the action with the divergence of the vortex vector;

$$\begin{aligned} \mathcal{S}_0[v(x)] = & \dots + \\ & 2 \int d^3x \int d^3y (\nabla \cdot v(x)) (h'(x-y) \cdot \eta_2 \cdot v(y)) \\ & + \int d^3x \int d^3y (\nabla \cdot v(x)) h''(x-y) (\nabla \cdot v(y)), \end{aligned} \quad (48)$$

Here $h'(x-y)$, and $h''(x-y)$ are from the b_1 terms in $H(q)$,

$$\begin{aligned} h'(x-y) & \equiv \int_{q \neq 0} \frac{d^3q}{(2\pi)^3} \frac{ib_1 G_0 \hat{q}}{q} e^{-iq(x-y)}, \\ h''(x-y) & \equiv \int_{q \neq 0} \frac{d^3q}{(2\pi)^3} \frac{b_1^2 G_0}{q^2} e^{-iq(x-y)}. \end{aligned} \quad (49)$$

Thus, the 3D vortex loop model with the 1D Berry phase term is given by a following generic form of the partition function,

$$\begin{aligned} Z = 1 + \sum_{n=1}^{\infty} \frac{1}{n!} \prod_{j=1}^n \left(\int_a^\infty \left(\frac{dl_j}{a_0} \right) t^{l_j} \int \left(\frac{d^3R_j}{a_0^3} \right) \int D\Omega_j(\lambda) \right) \exp \left[-2\pi i \chi \sum_{i=1}^n S_{12}^i \right. \\ \left. - \sum_{i,j=1}^n \oint_{\Gamma_i} \oint_{\Gamma_j} \left\{ dx^i \cdot dy^j F_1(x^i - y^j) + dx^i \cdot \eta_2 \cdot dy^j F_2(x^i - y^j) + dx^i \cdot G(x^i - y^j) \cdot dy^j \right\} \right]. \end{aligned} \quad (50)$$

The scalar functions $F_1(r)$ and $F_2(r)$ are the Fourier transforms of $F_1(q)$ and $F_2(q)$. A 3 by 3 symmetric matrix $G(r)$ is given by the scalar function $G_0(q)$;

$$G(r) \equiv \int \frac{d^3q}{(2\pi)^3} G_0(q) \eta_2 \hat{q} \hat{q}^T \eta_2 e^{-iq(x-y)}. \quad (51)$$

$F_1(r)$, $F_2(r)$ and $G(r)$ that emerge from the isotropic Coulomb potential [$F_1(r) \propto 1/|r|$, $F_2 = G = 0$] must be also algebraic functions of $|r_\perp|$ and r_0 with the same exponent. Such interaction potentials need the UV cutoff for the interaction length. We choose this UV cutoff in the same way as in Section II [see Eq. (13)],

$$\begin{aligned} & \oint_{\Gamma_i} \oint_{\Gamma_j} \left\{ dx^i \cdot dy^j \dots + dx^i \cdot \eta_2 \cdot dy^j \dots + \dots \right\} \\ & = \oint \oint_{|x^i - y^j| > a_0} \left\{ dx^i \cdot dy^j \dots + dx^i \cdot \eta_2 \cdot dy^j \dots + \dots \right\}. \end{aligned} \quad (52)$$

To analyze this action by a renormalization group method, we decompose the loop length integral in Eq. (50) into short-length region ($a < l_j < ab$) and long-length region ($ab < l_j$), and decompose the interaction in Eq. (52) into the short-distance part ($a_0 < |x^i - y^j| < a_0 b$) and the long-distance part ($a_0 b < |x^i - y^j|$). We expand the partition function up to the first order in the small $\ln b$. As in Section III, the vortex loop Γ in the short-length region is represented by a coplanar symmetric circle with its diameter a_0 ; $a = a_0 \pi$. To integrate out such short-loop DOF explicitly, we Taylor-expand the action in the power of the interaction between the short loop and others, while leaving the 1D Berry phase term on the shoulder of the exponential function;

$$\begin{aligned}
Z_v = & 1 + \left(\int_a^{ab} dl t^l \int_V d^3 R \int_{S_2} d^2 \Omega \right) e^{-s_1(\Gamma)} \\
& + \sum_{n=1}^{\infty} \frac{1}{n!} \prod_{j=1}^n \left(\int_{ab}^{\infty} dl_j t^{l_j} \int d^3 R_j \int D\Omega_j(\lambda) \right) e^{-\sum_{i=1}^n s_1(\Gamma_i) - \sum_{i,j=1}^n s_0(\Gamma_i, \Gamma_j)} \left\{ 1 - \sum_{j=1}^n \delta s_0(\Gamma_j) \right\} \\
& + \sum_{n=1}^{\infty} \frac{1}{n!} \prod_{j=1}^n \left(\int_{ab}^{\infty} dl_j t^{l_j} \int d^3 R_j \int D\Omega_j(\lambda) \right) e^{-\sum_{i=1}^n s_1(\Gamma_i) - \sum_{i,j=1}^n s_0(\Gamma_i, \Gamma_j)} \\
& \times \left(\int_a^{ab} dl t^l \int_V d^3 R \int_{S_2} d^2 \Omega \right) e^{-s_1(\Gamma)} \left\{ 1 - \left(\sum_{j=1}^n 2s_0(\Gamma, \Gamma_j) \right) + \frac{1}{2} \left(\sum_{j=1}^n 2s_0(\Gamma, \Gamma_j) \right)^2 + \dots \right\} \quad (53)
\end{aligned}$$

Here $s_1(\Gamma_j)$ and $s_0(\Gamma_i, \Gamma_j)$ are the 1D Berry phase term for the j -th loop, and the Coulombic interaction between the i -th and j -th loops, respectively;

$$s_1(\Gamma_j) \equiv 2\pi i \chi S_{12}^j, \quad (54)$$

$$\begin{aligned}
s_0(\Gamma_i, \Gamma_j) \equiv & \oint_{\Gamma_i} \oint_{\Gamma_j}^{a_0 b < |x^i - y^j|} \left\{ dx^i \cdot dy^j F_1(x^i - y^j) + \right. \\
& \left. dx^i \cdot \eta_2 \cdot dy^j F_2(x^i - y^j) + dx^i \cdot G(x^i - y^j) \cdot dy^j \right\}. \quad (55)
\end{aligned}$$

$\delta s_0(\Gamma_j)$ is the short-distance part of the Coulomb interaction within the j -th loop;

$$\begin{aligned}
\delta s_0(\Gamma_j) \equiv & \oint_{\Gamma_j} \oint_{a_0 < |x^j - y^j| < a_0 b} \left\{ dx^j \cdot dy^j F_1(x^j - y^j) + \right. \\
& \left. dx^j \cdot \eta_2 \cdot dy^j F_2(x^j - y^j) + dx^j \cdot G(x^j - y^j) \cdot dy^j \right\}. \quad (56)
\end{aligned}$$

As in section III, $s_0(\Gamma, \Gamma) \propto \ln b$ is omitted here, as its contribution appears with the higher power in $\ln b$. $\delta s_0(\Gamma_j)$ is on the order of $\ln b$, so that the partition function is further expanded up to the first order in $\delta s_0(\Gamma_j)$.

$\delta s_0(\Gamma_j)$ in Eq. (53) gives rise to 1-loop renormalization to the vortex fugacity parameter $\ln t$ [see Section IVC]. After an integration over the short-loop DOF [$\int_V d^3 R \int_{S_2} d^2 \Omega$], the first-order expansion term in $s_0(\Gamma, \Gamma_j)$ in the fourth term of Eq. (53) generates 1-loop renormalization to the Berry phase term $s_1(\Gamma_j)$ in the third term of Eq. (53)[Section IVD]. The second-order expansion term in $s_0(\Gamma, \Gamma_j)$ in the fourth term of Eq. (53) produces 1-loop renormalization to the interaction potentials $s_0(\Gamma_i, \Gamma_j)$ in the third term of Eq. (53)[Section IVE]. Note also that the second term as well as the zeroth-order in $s_0(\Gamma, \Gamma_j)$ of the fourth term can be included as an inhomogeneous part of the free-energy renormalization.

C. renormalization to vortex fugacity parameter

$\delta s_0(\Gamma_j)$ renormalizes the vortex fugacity parameter $\ln t$. To see this, note that the distance between the two

vortex-loop segments in δs_0 is a small quantity on the order of the lattice constant a_0 . Thus, we expand δs_0 in the power of the distance a_0 , keeping the leading order in the expansion;

$$\begin{aligned}
\delta s_0(\Gamma_j) = & \int_0^{l_j} d\lambda \int_{a_0 < |\lambda - \lambda'| < a_0 b} d\lambda' \\
& \left\{ \Omega_j(\lambda) \cdot \Omega_j(\lambda') F_1(x^j(\lambda) - x^j(\lambda')) + \dots \right\} \\
= & a_0 \ln b \int_0^{l_j} d\lambda \left\{ \Omega_j(\lambda) \cdot (\Omega_j(\lambda + a_0) \right. \\
& \left. + \Omega_j(\lambda - a_0)) F_1(\Omega_j(\lambda) a_0) + \mathcal{O}(a_0^2) \right\} + \dots \\
= & 2a_0 \ln b \int_0^{l_j} d\lambda \left\{ F_1(\Omega_j(\lambda) a_0) \right. \\
& \left. + \Omega_j(\lambda) \cdot \eta_2 \cdot \Omega_j(\lambda) F_2(\Omega_j(\lambda) a_0) + \right. \\
& \left. + \Omega_j(\lambda) \cdot G(\Omega_j(\lambda) a_0) \cdot \Omega_j(\lambda) \right\} + \dots \quad (57)
\end{aligned}$$

Here “...” in the last line denotes higher-order gradient expansion terms in a_0 , which renormalize other vortex loop parameters, e.g. the elastic energy parameter [See Section III]. Upon substitution into Eq. (53), the leading-order expansion term can be included as the renormalization to the vortex fugacity parameter;

$$\begin{aligned}
S_n e^{-\sum_{j=1}^n s_1(\Gamma_j) - \sum_{i,j=1}^n s_0(\Gamma_i, \Gamma_j)} & \left(1 - \sum_{k=1}^n \delta s(\Gamma_k) \right) \\
= S_n e^{-\sum_{j=1}^n s_1(\Gamma_j) - \sum_{i,j=1}^n s_0(\Gamma_i, \Gamma_j)} & \left(1 - 2a_0 \ln b \sum_{k=1}^n l_k \right. \\
& \left. \left\{ \langle F_1(\Omega a_0) \rangle_n + \langle \Omega \cdot \eta \cdot \Omega F_2(\Omega a_0) \rangle_n + \langle \Omega \cdot G(\Omega a_0) \cdot \Omega \rangle_n \right\} \right), \quad (58)
\end{aligned}$$

with

$$S_n \equiv \prod_{j=1}^n \left(\int_{ab}^{\infty} dl_j t^{l_j} \int d^3 R_j \int D\Omega_j(\lambda) \right). \quad (59)$$

Here $\langle \dots \rangle_n$ denotes a statistical average over all possible n vortex-loop configurations,

$$\langle F(\Omega a_0) \rangle_n \equiv \frac{\mathcal{S}_n e^{-\sum_{j=1}^n s_1 - \sum_{i,j=1}^n s_0} F(\Omega_k(\lambda) a_0)}{\mathcal{S}_n e^{-\sum_{j=1}^n s_1 - \sum_{i,j=1}^n s_0}}. \quad (60)$$

After the statistical average over the vortex-loop configurations, any function $F(\Omega_k(\lambda) a_0)$ of a tangential vector $\Omega_k(\lambda)$ at λ in the k -th vortex loop becomes independent of λ and from the loop index k . Thus, the integral over λ in the right-hand side of Eq. (57) can be safely taken, yielding a factor of loop length $[l_k]$ for each vortex loop. By the re-exponentiation, such $\langle \delta s(\Gamma_k) \rangle_n$ renormalizes the vortex fugacity parameter,

$$\begin{aligned} & \mathcal{S}_n e^{-\sum_{j=1}^n s_1(\Gamma_j) - \sum_{i,j=1}^n s_0(\Gamma_i, \Gamma_j)} \left(1 - \sum_{k=1}^n \delta s(\Gamma_k) \right) \\ &= \mathcal{S}_n e^{\ln(\bar{t}/t) \sum_{j=1}^n l_j - \sum_{j=1}^n s_1(\Gamma_j) - \sum_{i,j=1}^n s_0(\Gamma_i, \Gamma_j)}. \end{aligned} \quad (61)$$

Here the renormalized fugacity parameter \bar{t} is given by

$$\begin{aligned} \ln \bar{t} &= \ln t - 2a_0 \ln b \left\{ \langle F_1(\Omega a_0) \rangle_n \right. \\ &\quad \left. + \langle \Omega \cdot \eta \cdot \Omega F_2(\Omega a_0) \rangle_n + \langle \Omega \cdot G(\Omega a_0) \cdot \Omega \rangle_n \right\}. \end{aligned} \quad (62)$$

The renormalization to the fugacity parameter is generally dependent on a total number n of vortex loops, while its leading order expansion in the power of a_0/T becomes independent of n . Namely, as F_1 , F_2 , and G are quantities on the order of $1/T$, they can be treated as small quantities, allowing a perturbative evaluation of the statistical average in the power of a_0/T ;

$$\begin{aligned} \langle f(\Omega a_0) \rangle_n &= \frac{\mathcal{S}_n e^{-\sum_{j=1}^n s_1(\Gamma_j)} f(\Omega_k(\lambda) a_0)}{\mathcal{S}_n e^{-\sum_{j=1}^n s_1(\Gamma_j)}} + \mathcal{O}(a_0 F_j f) \\ &\equiv \langle f(\Omega a_0) \rangle + \dots, \end{aligned} \quad (63)$$

with

$$\begin{aligned} \langle f(\Omega a_0) \rangle &\equiv \frac{\int dl t^l \int d^3 R \int D\Omega(\lambda) e^{-s_1(\Gamma)} f(\Omega(\lambda) a_0)}{\int dl t^l \int d^3 R \int D\Omega(\lambda) e^{-s_1(\Gamma)}} \\ &= \frac{\int dl t^l \int D\Omega(\lambda) e^{-s_1(\Gamma)} f(\Omega(\lambda) a_0)}{\int dl t^l \int D\Omega(\lambda) e^{-s_1(\Gamma)}}. \end{aligned} \quad (64)$$

Importantly, the leading order term, Eq. (64), is given by a statistical average over the configuration of a single vortex loop; it is independent of the number n . This gives the one-loop renormalization to the fugacity parameter,

$$\begin{aligned} \ln \bar{t} &= \ln t - 2a_0 \ln b \left\{ \langle F_1(\Omega a_0) \rangle \right. \\ &\quad \left. + \langle \Omega \cdot \eta \cdot \Omega F_2(\Omega a_0) \rangle + \langle \Omega \cdot G(\Omega a_0) \cdot \Omega \rangle \right\}. \end{aligned} \quad (65)$$

In Section IVF, Eq. (64) will be evaluated with a further approximation [see Eq. (126)].

D. renormalization to 1D Berry phase term

An integration over the short-loop DOF makes the first-order expansion terms in $s_0(\Gamma, \Gamma_j)$ in the fourth term of Eq. (53) into the renormalization to the 1D Berry phase term. To see this, we consider the short loop Γ as the circular loop with its diameter a_0 , and expand $s_0(\Gamma, \Gamma_j)$ in the power of the diameter a_0 of the short loop,

$$\begin{aligned} s_0(\Gamma, \Gamma_j) &= \frac{a_0^2 \pi}{4} \Omega_\mu \epsilon_{\mu\lambda\phi} \oint_{\Gamma_j} \left\{ dy_\phi^j \nabla_{R_\lambda} F_1(R - y^j) \right. \\ &\quad \left. + dy_\phi^j (\eta_2)_{\phi\psi} \nabla_{R_\lambda} F_2(R - y^j) + dy_\psi^j \nabla_{R_\lambda} G_{\phi\psi}(R - y^j) \right\}. \end{aligned} \quad (66)$$

The coplanar and circular loop Γ is parameterized by its center-of-mass coordinate R , and a unit vector $\Omega \equiv (\cos \psi \sin \theta, \sin \psi \sin \theta, \cos \theta)$ normal to the coplanar plane. An integration of the leading-order gradient term in Eq. (66) over Ω gives out

$$\begin{aligned} & \int_{S_2} d^2 \Omega e^{-s_1(\Gamma)} \sum_j 2s_0(\Gamma, \Gamma_j) \\ &= 2i(a_0\pi)^2 \frac{\partial}{\partial \nu} \left(\frac{\sin \nu}{\nu} \right) \epsilon_{0\lambda\phi} \sum_j \oint_{\Gamma_j} \nabla_{R_\lambda} \left(dy_\phi^j F_1(R - y^j) \right. \\ &\quad \left. + dy_\phi^j (\eta_2)_{\phi\psi} F_2(R - y^j) + dy_\psi^j G_{\phi\psi}(R - y^j) \right) \\ &= 2i(\dots) \sum_j \epsilon_{0\lambda\phi} \epsilon_{\xi\eta\psi} \int_{S_j} dn_\xi \nabla_{R_\lambda} \nabla_{y_n^j} \left(\delta_{\phi\psi} F_1(R - y^j) \right. \\ &\quad \left. + (\eta_2)_{\phi\psi} F_2(R - y^j) + G_{\phi\psi}(R - y^j) \right), \end{aligned} \quad (67)$$

where $s_1(\Gamma) \equiv i\nu \cos \theta$ and $\nu \equiv \frac{\pi^2 a_0^2}{2} \chi$. From the 2nd line to the third line, the line integral with respect to y^j along Γ_j is transformed into a surface integral with respect to y^j over an open surface S_j , by the Stokes' theorem. Namely, the open surface S_j is encompassed by $\Gamma_j \equiv \partial S_j$. dn is a vector normal to S_j at y^j , where dn and the vorticity of Γ_j obey the right-handed rule.

An integration over the center-of-mass coordinate R makes Eq. (67) into a quantity proportional to the pro-

jected area S_{12}^j for each closed loop Γ_j ,

$$\begin{aligned}
& \int_V d^3 R \int_{S_2} d^2 \Omega e^{-s_1(\Gamma)} \sum_j 2s_0(\Gamma, \Gamma_j) \\
&= -2i(\dots) \sum_j \epsilon_{0\lambda\phi} \epsilon_{\xi\eta\psi} \int_{S_j} dn_\xi \int_V d^3 R \nabla_{R_\lambda} \nabla_{R_\eta} \\
&\quad \left(\delta_{\phi\psi} (F_1(R - y^j) + F_2(R - y^j)) + G_{\phi\psi}(R - y^j) \right) \\
&= -2i(\dots) \sum_j (\delta_{0\xi} \delta_{\lambda\eta} - \delta_{0\eta} \delta_{\lambda\xi}) \int_{S_j} dn_\xi \int_V d^3 R \\
&\quad \nabla_{R_\lambda} \nabla_{R_\eta} (F_1(R - y^j) + F_2(R - y^j)) \\
&= -2i(\dots) \sum_{j=1}^n \int_V d^3 R \\
&\quad \left(\int_{S_j} dn_0 \nabla_{R_\lambda}^2 (F_1(R - y^j) + F_2(R - y^j)) \right. \\
&\quad \left. - \int_{S_j} dn_\lambda \nabla_{R_0} \nabla_{R_\lambda} (F_1(R - y^j) + F_2(R - y^j)) \right) \\
&= -2i(a_0\pi)^2 \frac{\partial}{\partial\nu} \left(\frac{\sin\nu}{\nu} \right) \\
&\quad \times \int_V d^3 R (\nabla_{R_1}^2 + \nabla_{R_2}^2) (F_1(R) + F_2(R)) \sum_{j=1}^n S_{12}^j. \tag{68}
\end{aligned}$$

From Eq. (67) to the second line, we use $\nabla_y = -\nabla_R$ and $\epsilon_{0\lambda\phi}(\eta_2)_{\phi\psi} = \epsilon_{0\lambda\phi}\delta_{\phi\psi}$. From the second line to the third line, G term is dropped from the integrand. This is because for $\xi = 0$, the Fourier-transform of the G term is zero ;

$$\begin{aligned}
& \epsilon_{0\lambda\phi} \epsilon_{0\eta\psi} \nabla_{R_\lambda} \nabla_{R_\eta} G_{\phi\psi}(R) \\
&= - \int \frac{d^3 q}{(2\pi)^3} \epsilon_{0\lambda\phi} \epsilon_{0\eta\psi} q^2 \hat{q}_\lambda \hat{q}_\eta \hat{q}_\phi \hat{q}_\psi G(q) e^{-iqR} = 0. \tag{69}
\end{aligned}$$

For $\xi = 1, 2$, the G term is odd under the π -rotation around the x_0 axis [Eq. (43)], and the R -integral of such term is zero. By the same reason, $\nabla_{R_0} \nabla_{R_\lambda} (F_1 + F_2)$ for $\lambda = 1, 2$ is also removed from the integrand in the fourth line. Finally, the right-handed rule between dn and the vorticity of Γ_j equates $\int_{S_j} dn_0$ with S_{12}^j in the last line.

Such imaginary number in Eq. (68) can be included as a renormalization to the 1D Berry term in the third term of Eq. (53);

$$\mathcal{S} e^{-\sum_j s_1(\Gamma_j)} \left\{ 1 - \left(\int_a^{ab} dt t^l \int_V d^3 R \int_{S_2} d^2 \Omega \right) e^{-s_1(\Gamma)} \left(\sum_j 2s_0(\Gamma, \Gamma_j) \right) \right\} = \mathcal{S} e^{-\sum_j \bar{s}_1(\Gamma_j)}, \tag{70}$$

with

$$\mathcal{S} \equiv \sum_{n=1}^{\infty} \frac{1}{n!} \prod_{j=1}^n \left(\int_{ab}^{\infty} dl_j t^{l_j} \int d^3 R_j \int D\Omega_j(\lambda) \right). \tag{71}$$

Here $\bar{s}_1(\Gamma_j) = i2\pi\bar{\chi}S_{12}^j$, and

$$\begin{aligned}
\bar{\chi} &\equiv \chi - \ln b a t^a a_0^2 \pi \frac{\partial}{\partial\nu} \left(\frac{\sin\nu}{\nu} \right) \\
&\quad \int_V d^3 R (\nabla_{R_1}^2 + \nabla_{R_2}^2) (F_1(R) + F_2(R)), \tag{72}
\end{aligned}$$

with $a = a_0\pi$. For the isotropic Coulomb interac-

tion [$F_1(R) = 1/|R|$, $F_2(R) = G(R) = 0$], $(\nabla_{R_1}^2 + \nabla_{R_2}^2)F_1(R) = -\frac{8\pi}{3}\delta(R)$, so that the 1-loop renormalization to χ takes a negative value for small χ (ν). For slightly general forms of $F_1(R)$ and $F_2(R)$ [see Eq. (116)], the 1-loop renormalization to χ is also negative for small χ . Thanks to this negative value, the 1D Berry phase term is always renormalized to zero near a high- T fixed point with divergent fugacity t [see Section IVG].

E. renormalization to Coulomb interaction potentials

An integration over the short-loop DOF transforms the second-order expansion term in $s_0(\Gamma, \Gamma_j)$ in the fourth term of Eq. (53) into 1-loop renormalizations to the three types of interaction potentials;

$$\mathcal{S} e^{-\sum_{i,j=1}^n s_0(\Gamma_i, \Gamma_j)} \left\{ 1 + \left(\int_a^{ab} dt t^l \int_V d^3 R \int_{S_2} d^2 \Omega \right) e^{-s_1(\Gamma)} \frac{1}{2} \left(\sum_{j=1}^n 2s_0(\Gamma, \Gamma_j) \right)^2 \right\} = \mathcal{S} e^{-\sum_{i,j} \bar{s}_0(\Gamma_i, \Gamma_j)}. \tag{73}$$

To determine $\bar{s}_0(\Gamma_i, \Gamma_j)$ thus introduced, take the Ω -integral of a square of Eq. (66) with $s_1(\Gamma) = i\nu \cos \theta$. The squaring yields 6 different couplings among F_1 , F_2 , and G , where all the couplings share the same Ω -integration,

$$\begin{aligned} & \int_{S_2} d^2\Omega e^{-i\nu \cos \theta} \Omega_\mu \Omega_\psi \epsilon_{\mu\lambda\phi} \epsilon_{\psi\rho\sigma} \\ &= \frac{4\pi}{3} \epsilon_{\mu\lambda\phi} \epsilon_{\mu\rho\sigma} (d_1 \delta_{\mu\mu} + d_2 (\eta_2)_{\mu\mu}) \\ &= \frac{4\pi}{3} d_1 (\delta_{\lambda\rho} \delta_{\phi\sigma} - \delta_{\lambda\sigma} \delta_{\phi\rho}) + \frac{4\pi}{3} d_2 (- (\eta_2)_{\lambda\rho} \delta_{\phi\sigma} \\ & \quad - \delta_{\lambda\rho} (\eta_2)_{\phi\sigma} + (\eta_2)_{\lambda\sigma} \delta_{\phi\rho} + \delta_{\lambda\sigma} (\eta_2)_{\phi\rho}). \end{aligned} \quad (74)$$

Here d_1 and d_2 are functions of the 1D Berry phase parameter $\nu \equiv \frac{a_0^2 \pi^2}{2} \chi$;

$$\begin{aligned} d_1 &\equiv \frac{\sin \nu}{\nu}, \\ d_2 &\equiv -\frac{\sin \nu}{\nu} + \frac{3(\sin \nu - \nu \cos \nu)}{\nu^3}. \end{aligned} \quad (75)$$

In the non-topological limit ($\nu = 0$), $d_1 = 1$ and $d_2 = 0$. For small ν , $0 < d_1 < 1$ and $d_2 > 0$.

In the next subsection, we will first calculate the square of $F_1(r)$, and show that due to the 1D Berry phase term, screening effects by unpolarized vortex loops are generally suppressed, and the $F_1 \times F_1$ screening by polarized vortex loop induces spatial anisotropy in the $F_1(r)$ interaction, such that a characteristic length scale along the topological (x_0) direction becomes longer than the length scale along the other two directions. We also show that the $F_1 \times F_1$ screening by the polarized loops generates the $F_2(r)$ interaction.

1. $\nabla_R F_1(R - x^i) \times \nabla_R F_1(R - y^j)$

A coupling between $\nabla_{R_\lambda} F_1(R - x^i)$ and $\nabla_{R_\rho} F_1(R - y^j)$ in $\frac{1}{2} (\sum_j 2s_0(\Gamma, \Gamma_j))^2$ is given by

$$\begin{aligned} & \int_V d^3R \int_{S_2} d^2\Omega e^{-s_1(\Gamma)} \sum_{i=1}^n \sum_{j=1}^n \oint_{\Gamma_i} dx_\phi^i \oint_{\Gamma_j} dy_\sigma^j \frac{a_0^4 \pi^2}{8} \\ & \quad \Omega_\mu \Omega_\psi \epsilon_{\mu\lambda\phi} \epsilon_{\psi\rho\sigma} \left(\nabla_{R_\lambda} F_1(R - x^i) \right) \left(\nabla_{R_\rho} F_1(R - y^j) \right) \\ &= \frac{a_0^4 \pi^3}{6} \sum_{i,j} \epsilon_{\mu\lambda\phi} \epsilon_{\mu\rho\sigma} (d_1 \delta_{\mu\mu} + d_2 (\eta_2)_{\mu\mu}) \int_V d^3R \\ & \quad \oint_{\Gamma_i} dx_\phi^i \oint_{\Gamma_j} dy_\sigma^j \left(\nabla_{R_\lambda} F_1(R - x^i) \right) \left(\nabla_{R_\rho} F_1(R - y^j) \right). \end{aligned} \quad (76)$$

When using the second line of Eq. (74), note that terms with a factor of $\delta_{\lambda\sigma}$ or $\delta_{\phi\rho}$ in its right hand side reduce to zero in the partition function with closed vortex loops. This is because they all appear in the action \mathcal{S}_0 with the divergence of the vortex vector. For example, a term

with the factor of $\delta_{\lambda\sigma}$ in Eq. (74) reduces to zero after integration by parts;

$$\begin{aligned} & \int_V d^3R \oint_{\Gamma_i} dx_\phi^i \left(\nabla_{R_\sigma} F_1(R - x^i) \right) \\ & \quad \times \oint_{\Gamma_j} dy_\sigma^j \left(\nabla_{R_\rho} F_1(R - y^j) \right) \\ &= \int_V d^3R \oint_{\Gamma_i} dx_\phi^i F_1(R - x^i) \\ & \quad \times \oint_{\Gamma_j} dy_\sigma^j \nabla_{y_\sigma^j} \left(\left(\nabla_{R_\rho} (F_1(R - y^j)) \right) \right) = 0. \end{aligned} \quad (77)$$

The rest of terms in Eq. (76) are summarized into two types of the interaction potentials,

$$\begin{aligned} & \int_V d^3R \int_{S_2} d^2\Omega e^{-s_1(\Gamma)} \sum_{i,j} \oint_{\Gamma_i} dx_\phi^i \oint_{\Gamma_j} dy_\sigma^j \frac{a_0^4 \pi^2}{8} \\ & \quad \Omega_\mu \Omega_\psi \epsilon_{\mu\lambda\phi} \epsilon_{\psi\rho\sigma} \left(\nabla_{R_\lambda} F_1(R - x^i) \right) \left(\nabla_{R_\rho} F_1(R - y^j) \right) \\ &= \sum_{i,j=1}^n \oint_{\Gamma_i} \oint_{\Gamma_j} \left(dx^i \cdot dy^j c_{111}(x^i - y^j) \right. \\ & \quad \left. + dx^i \cdot \eta_2 \cdot dy^j c_{112}(x^i - y^j) \right), \end{aligned} \quad (78)$$

with

$$\begin{aligned} c_{111}(x^i - y^j) &\equiv \frac{a_0^4 \pi^3}{6} (d_1 \delta_{\lambda\lambda} - d_2 (\eta_2)_{\lambda\lambda}) \int_V d^3R \\ & \quad \left(\nabla_{R_\lambda} F_1(R - x^i) \right) \left(\nabla_{R_\lambda} F_1(R - y^j) \right), \quad (79) \\ c_{112}(x^i - y^j) &\equiv \frac{a_0^4 \pi^3}{6} (-d_2) \delta_{\lambda\lambda} \int_V d^3R \\ & \quad \left(\nabla_{R_\lambda} F_1(R - x^i) \right) \left(\nabla_{R_\lambda} F_1(R - y^j) \right). \end{aligned} \quad (80)$$

Upon a substitution of Eq. (78) into Eq.(73), $c_{111}(r)$ and $c_{112}(r)$ generate renormalization to $F_1(r)$ and $F_2(r)$ in $\bar{s}_0(\Gamma_i, \Gamma_j)$;

$$\bar{F}_1(r) \equiv F_1(r) - a t^a (c_{111}(r) + \dots) \ln b, \quad (81)$$

$$\bar{F}_2(r) \equiv F_2(r) - a t^a (c_{112}(r) + \dots) \ln b. \quad (82)$$

Note that the convolution in Eqs. (79,80) are most conveniently expressed by products in the q space;

$$c_{111}(q) = \frac{a_0^4 \pi^3}{6} (d_1 q^2 - d_2 (\eta_2)_{\lambda\lambda} q_\lambda^2) F_1^2(q), \quad (83)$$

$$c_{112}(q) = \frac{a_0^4 \pi^3}{6} (-d_2) q^2 F_1^2(q), \quad (84)$$

with $F_1(-q) = F_1(q)$. So is the 1-loop renormalization to F_1 and F_2 ,

$$\bar{F}_1(q) \equiv F_1(q) - a t^a (c_{111}(q) + \dots) \ln b, \quad (85)$$

$$\bar{F}_2(q) \equiv F_2(q) - a t^a (c_{112}(q) + \dots) \ln b. \quad (86)$$

In the limit of $\nu = 0$, the first equation reduces to Eq. (29) with $F_1(q) = 2\pi^2/(Tq^2)$. In the presence of small ν , $c_{111}(q)$ induces spatial anisotropy in the F_1 interaction, e.g. $F_1^{-1}(q) = Tq^2/(2\pi^2) \rightarrow Tq^2/(2\pi^2) + C \ln b((d_1 - d_2)q_1^2 + (d_1 + 2d_2)q_0^2)$ with a positive constant $C = a_0\pi^4 t^a/6$ [Here we also recovered the normalization factor of the l_j -integral and R -integral]. Since $d_2 > 0$ for smaller ν , the positive C suggests an enhancement of a ratio of a length scale along the 0 axis to a length scale along the others. This indicates that the small 1D Berry phase term elongates the characteristic length scale along the x_0 axis, being consistent with the phase interference argument in Section IVA. For the small ν , $c_{112}(q)$ in the second equation induces the $F_2(r)$ interaction with a positive coefficient and $1/r$ decay. A short-distance part of such $F_2(r)$ interaction favors vortex-loop segments polarized along the x_0 axis, being also consistent with the argument in Section IVA.

In the next subsection, we will calculate the coupling between $F_1(r)$ and $F_2(r)$, and show that the $F_1 \times F_2$ screening by polarized vortex loops induces the dipolar-type $G(r)$ interaction, helping to confine vortex loops within planes parallel to the topological (x_0) direction. We also show that the $F_1 \times F_2$ screening by the polarized vortex loops induces the spatial anisotropy in the $F_2(r)$ interaction, such that a characteristic length scale along the topological (x_0) direction becomes longer than the other length scale.

2. $\nabla_R F_1(R - x^i) \times \nabla_R F_2(R - y^j)$

A coupling between $\nabla_{R_\lambda} F_1(R - x^i)$ and $\nabla_{R_\rho} F_2(R - y^j)$ in $\frac{1}{2}(\sum_j 2s_0(\Gamma, \Gamma_j))^2$ is summarized by

$$\begin{aligned} & \int_V d^3 R \int_{S_2} d^2 \Omega e^{-s_1(\Gamma)} \sum_{i,j=1}^n \oint_{\Gamma_i} dx_\phi^i \oint_{\Gamma_j} dy_\sigma^j (\eta_2)_{\sigma\sigma} \frac{a_0^4 \pi^2}{4} \\ & \Omega_\mu \Omega_\psi \epsilon_{\mu\lambda\phi} \epsilon_{\psi\rho\sigma} \left(\nabla_{R_\lambda} F_1(R - x^i) \right) \left(\nabla_{R_\rho} F_2(R - y^j) \right) \\ & = \frac{a_0^4 \pi^3}{3} \sum_{i,j} \epsilon_{\mu\lambda\phi} \epsilon_{\mu\rho\sigma} (d_1 \delta_{\mu\mu} + d_2 (\eta_2)_{\mu\mu}) \\ & \quad \int_V d^3 R \oint_{\Gamma_i} dx_\phi^i \oint_{\Gamma_j} dy_\sigma^j (\eta_2)_{\sigma\sigma} \\ & \quad \left(\nabla_{R_\lambda} F_1(R - x^i) \right) \left(\nabla_{R_\rho} F_2(R - y^j) \right) \end{aligned} \quad (87)$$

Multiplication of Eq. (74) by η_2 with $\eta_2^2 = -\eta_2 + 2$ facilitates a subsequent calculation of Eq. (87),

$$\begin{aligned} & \epsilon_{\mu\lambda\phi} \epsilon_{\mu\rho\sigma} (d_1 \delta_{\mu\mu} + d_2 (\eta_2)_{\mu\mu}) (\eta_2)_{\sigma\sigma} \\ & = d_1 (\delta_{\lambda\rho} (\eta_2)_{\phi\sigma} - (\eta_2)_{\lambda\sigma} \delta_{\phi\rho}) + d_2 (- (\eta_2)_{\lambda\rho} (\eta_2)_{\phi\sigma} \\ & \quad - \delta_{\lambda\rho} (\eta_2)_{\phi\sigma} + (\eta_2)_{\lambda\sigma} \delta_{\phi\rho} + (\eta_2)_{\lambda\sigma} (\eta_2)_{\phi\rho}) \\ & = -2d_2 (\delta_{\lambda\rho} \delta_{\phi\sigma} - \delta_{\lambda\sigma} \delta_{\phi\rho}) \\ & \quad + (d_1 + d_2) (\delta_{\lambda\rho} (\eta_2)_{\phi\sigma} - (\eta_2)_{\lambda\sigma} \delta_{\phi\rho}) \\ & \quad + d_2 (- (\eta_2)_{\lambda\rho} (\eta_2)_{\phi\sigma} + (\eta_2)_{\lambda\sigma} (\eta_2)_{\phi\rho}). \end{aligned} \quad (88)$$

Note that terms with a factor of $\delta_{\lambda\sigma}$ or $\delta_{\phi\rho}$ in the right hand side of Eq. (88) reduce to zero after the integration by parts. The rest of the terms in Eq. (88) are summarized into the three types of interaction potentials,

$$\begin{aligned} & \int_V d^3 R \int_{S_2} d^2 \Omega e^{-s_1(\Gamma)} \sum_{i,j=1}^n \oint_{\Gamma_i} dx_\phi^i \oint_{\Gamma_j} dy_\sigma^j (\eta_2)_{\sigma\sigma} \frac{a_0^4 \pi^2}{4} \\ & \Omega_\mu \Omega_\psi \epsilon_{\mu\lambda\phi} \epsilon_{\psi\rho\sigma} \left(\nabla_{R_\lambda} F_1(R - x^i) \right) \left(\nabla_{R_\rho} F_2(R - y^j) \right) \\ & = \sum_{i,j} \oint_{\Gamma_i} \oint_{\Gamma_j} \left(dx^i \cdot dy^j c_{121}(x^i - y^j) + \right. \\ & \quad \left. dx^i \cdot \eta_2 \cdot dy^j c_{122}(x^i - y^j) + \right. \\ & \quad \left. dx^i \cdot c_{120}(x^i - y^j) \cdot dy^j \right), \end{aligned} \quad (89)$$

with

$$\begin{aligned} c_{121}(x^i - y^j) & \equiv \frac{a_0^4 \pi^3}{3} (-2d_2) \delta_{\lambda\lambda} \\ & \int_V d^3 R \left(\nabla_{R_\lambda} F_1(R - x^i) \right) \left(\nabla_{R_\lambda} F_2(R - y^j) \right), \end{aligned} \quad (90)$$

$$\begin{aligned} c_{122}(x^i - y^j) & \equiv \frac{a_0^4 \pi^3}{3} \left((d_1 + d_2) \delta_{\lambda\lambda} - d_2 (\eta_2)_{\lambda\lambda} \right) \\ & \int_V d^3 R \left(\nabla_{R_\lambda} F_1(R - x^i) \right) \left(\nabla_{R_\lambda} F_2(R - y^j) \right), \end{aligned} \quad (91)$$

$$\begin{aligned} (c_{120})_{\phi\sigma}(x^i - y^j) & \equiv \frac{a_0^4 \pi^3}{3} d_2 (\eta_2)_{\phi\rho} (\eta_2)_{\lambda\sigma} \\ & \int_V d^3 R \left(\nabla_{R_\lambda} F_1(R - x^i) \right) \left(\nabla_{R_\rho} F_2(R - y^j) \right). \end{aligned} \quad (92)$$

When Eq. (89) is substituted into Eq. (73), $c_{121}(r)$ and $c_{122}(r)$ give renormalizations to $F_1(r)$ and $F_2(r)$, while $c_{120}(r)$ induces a renormalization to $G(r)$. In fact, in momentum space, the induced interactions take the same forms as $F_1(q)$, $F_2(q)$, and $G(q)$, respectively;

$$c_{121}(q) = \frac{a_0^4 \pi^3}{3} (-2d_2) q^2 F_1(q) F_2(q), \quad (93)$$

$$c_{122}(q) = \frac{a_0^4 \pi^3}{3} (d_1 q^2 + 3d_2 q_0^2) F_1(q) F_2(q), \quad (94)$$

$$\begin{aligned} (c_{120})_{\phi\sigma}(q) & = \frac{a_0^4 \pi^3}{3} d_2 q^2 F_1(q) F_2(q) (\eta_2 \hat{q} \hat{q}^T \eta_2)_{\phi\sigma} \\ & \equiv c_{120}(q) (\eta_2 \hat{q} \hat{q}^T \eta_2)_{\phi\sigma}. \end{aligned} \quad (95)$$

Thus,

$$\bar{F}_1(q) \equiv F_1(q) - a t^a (c_{111}(q) + c_{121}(q) + \dots) \ln b, \quad (96)$$

$$\bar{F}_2(q) \equiv F_2(q) - a t^a (c_{112}(q) + c_{122}(q) + \dots) \ln b, \quad (97)$$

$$\bar{G}_0(q) = G_0(q) - a t^a (c_{120}(q) + \dots) \ln b. \quad (98)$$

For $F_1(r) = F_2(r) = 1/|r|$, the induced $G(r)$ potential takes a form of a dipole-dipole interaction modulated by η_2 ,

$$\begin{aligned} g(r) & \propto -d_2 \int_{q \neq 0} \frac{d^3 q}{(2\pi)^3} e^{-iqr} \eta_2 \frac{\hat{q} \hat{q}^T}{q^2} \eta_2 \\ & = -\frac{\pi d_2}{2} \eta_2 \left(\frac{1 - \hat{r} \hat{r}^T}{|r|} \right) \eta_2. \end{aligned} \quad (99)$$

Note that two endpoints of an open vortex line are attracted by a linear confining potential [see Appendix A] [30]. Since the endpoint and vortex-loop segment can be regarded as magnetic monopoles and associated magnetic dipoles respectively, the form of $(1 - \hat{r}\hat{r}^T)/|r|$ in the right-hand side is interpreted as the dipole-dipole interaction that can be derived from the second-order derivatives of the linear confining potential. The induced $g(r)$ interaction characterizes the energetics of curved vortex loops. Due to the modulation factor η_2 , it favors those

vortex loops curving within the x_1 - x_0 or x_2 - x_0 planes, while disfavoring those loops curving within the x_1 - x_2 plane. In other words, the induced $g(r)$ helps to confine the vortex loops in a plane parallel to the x_0 axis, being consistent with the phase interference argument in Section IVA.

Other couplings in $2(\sum_j s_0(\Gamma, \Gamma_j))^2$ are also calculated in Appendix B. Together with the results, Eqs. (61,70,73) give the partition function after the integration of the short-loop DOF,

$$Z_v = e^{4\pi V \frac{\sin \nu}{\nu} a t^\alpha \ln b} \left(1 + \sum_{n=1}^{\infty} \frac{1}{n!} \prod_{j=1}^n \left(\int_{ab}^{\infty} dl_j \int d^3 R_j \int D\Omega_j(\lambda) \right) e^{-i2\pi\bar{\chi} \sum_{j=1}^n S_{12}^j - \sum_{i,j=1}^n \bar{s}_0(\Gamma_i, \Gamma_j) + \sum_{j=1}^n l_j \ln \bar{t}} \right) \quad (100)$$

$$\bar{s}_0(\Gamma_i, \Gamma_j) \equiv \oint_{\Gamma_i} \oint_{\Gamma_j}^{a_0 b < |x^i - y^j|} \left\{ dx^i \cdot dy^j \bar{F}_1(x^i - y^j) + dx^i \cdot \eta_2 dy^j \bar{F}_2(x^i - y^j) + dx^i \cdot \bar{G}(x^i - y^j) \cdot dy^j \right\}. \quad (101)$$

Here \bar{t} and $\bar{\chi}$ are given by Eqs. (64,65) and Eq. (72) respectively. The Fourier transforms of $\bar{F}_1(r)$, $\bar{F}_2(r)$, and $\bar{G}(r)$ are given by

$$\bar{F}_1(q) \equiv F_1(q) - a t^\alpha (c_{111}(q) + c_{121}(q) + c_{221}(q)) \ln b \quad (102)$$

$$\bar{F}_2(q) \equiv F_2(q) - a t^\alpha (c_{112}(q) + c_{122}(q) + c_{222}(q)) \ln b \quad (103)$$

$$\bar{G}_0(q) \equiv G_0(q) - a t^\alpha (c_{120}(q) + c_{220}(q) + c_{100}(q) + c_{200}(q) + c_{000}(q)) \ln b, \quad (104)$$

with Eq. (51). $c_{ijk}(q)$ is given by Eqs. (83,84, 93,94,95, B7,B8,B9,B11,B13,B15).

After the length rescaling of Eq. (14),

$$\begin{aligned} q' &= qb, \quad S_{12}^{j'} = S_{12}^j b^{-2}, \quad \chi' = \bar{\chi} b^2, \\ F_j'(q') &= \bar{F}_j(q) b^{-1}, \quad F_j'(r') = \bar{F}_j(r) b^2, \end{aligned} \quad (105)$$

we obtain closed RG equations for $F_1(q)$, $F_2(q)$, $G_0(q)$, $\ln t$ and χ . The RG equations are most conveniently given with proper normalizations. Firstly, normalize $F_j(q)$ ($j = 1, 2$) and $G_0(q)$ by $q^2 \equiv q_1^2 + q_2^2 + q_0^2$,

$$\begin{aligned} F_j(q) &\equiv \frac{4\pi}{q^2} f_j(\hat{q}), \\ G_0(q) &\equiv \frac{4\pi}{q^2} g_0(\hat{q}). \end{aligned} \quad (106)$$

Here $f_j(\hat{q})$ and $g_0(\hat{q})$ depend only on $\hat{q} \equiv q/|q|$, and they correspond to $\frac{\pi}{2T}$ in Section III, sharing the same tree-level scaling dimension with $1/T$; $f_j'(\hat{q}) = \bar{F}_j(\hat{q}) b$. As their dimension is an inverse of the length, we further normalize them by the UV cutoff length scale a_0 ;

$$\begin{aligned} y_j(\hat{q}) &\equiv a_0 f_j(\hat{q}), \\ y_0(\hat{q}) &\equiv a_0 g_0(\hat{q}). \end{aligned} \quad (107)$$

The normalized functions $y_j(\hat{q})$ correspond to $\frac{a_0 \pi}{2T}$ in Section III. From $y_j(\hat{q})$, we define three functions $Y_j(r)$

($j = 1, 2, 0$) that correspond to $F_j(r)$ ($j = 1, 2$) and $G_0(r)$ respectively;

$$\begin{aligned} Y_j(r) &\equiv \int \frac{d^3 q}{(2\pi)^3} \frac{4\pi}{q^2} y_j(\hat{q}) e^{-iqr} = a_0 F_j(r), \\ Y_0(r) &\equiv \int \frac{d^3 q}{(2\pi)^3} \frac{4\pi}{q^2} y_0(\hat{q}) \eta_2 \hat{q} \hat{q}^T \eta_2 e^{-iqr} \\ &= a_0 G(r). \end{aligned} \quad (108)$$

The functional RG equations for $x \equiv a_0 \ln t$, $\nu \equiv \frac{a_0^2 \pi^2}{2} \chi$,

$y_j(\hat{q})$ and $Y_j(r)$ ($j = 1, 2, 0$) are given by;

$$\frac{dx}{d \ln b} = x - 2 \left\{ \langle Y_1(\Omega) \rangle + \langle \Omega \cdot \eta_2 \cdot \Omega Y_2(\Omega) \rangle + \langle \Omega \cdot Y_0(\Omega) \cdot \Omega \rangle \right\}, \quad (109)$$

$$\frac{d\nu}{d \ln b} = 2\nu - \frac{3\Delta}{4} \frac{\partial}{\partial \nu} \left(\frac{\sin \nu}{\nu} \right) \times \int_V d^3 r \nabla_{r_\perp}^2 (Y_1(r) + Y_2(r)), \quad (110)$$

$$\frac{dy_1}{d \ln b} = y_1 - \Delta \left\{ (d_1 - d_2 \hat{q}_\perp^2 (\eta_2)_{\lambda\lambda}) y_1^2 - 4d_2 y_1 y_2 + (2d_1 + 6d_2 \hat{q}_0^2) y_2^2 \right\}, \quad (111)$$

$$\frac{dy_2}{d \ln b} = y_2 - \Delta \left\{ -d_2 y_1^2 + (2d_1 + 6d_2 \hat{q}_0^2) y_1 y_2 - (d_1 + d_2 (2 + 3\hat{q}_0^2)) y_2^2 \right\}, \quad (112)$$

$$\frac{dy_0}{d \ln b} = y_0 - \Delta \left\{ 2d_2 y_1 y_2 - (d_1 + 2d_2) y_2^2 + 2(d_1 + d_2) y_1 y_0 - 2(d_1 + d_2) (2\hat{q}_\perp^2 - \hat{q}_0^2) y_2 y_0 + 9(d_1 + d_2) \hat{q}_\perp^2 \hat{q}_0^2 y_0^2 \right\}, \quad (113)$$

with $\Delta \equiv \frac{2\pi^5}{3} e^{\pi x}$, and $\hat{q}_\perp^2 \equiv \hat{q}_1^2 + \hat{q}_2^2$. d_1 and d_2 are functions of the normalized Berry phase parameter ν [See Eqs. (75)]. The functional RG equation indicates that the initial isotropic Coulomb interaction [$y_1 = \frac{\pi a_0}{2T}$, $y_2 = y_0 = 0$] induces $y_2(\hat{q})$ and $y_0(\hat{q})$ with spatial anisotropies, and the induced $y_j(\hat{q})$ ($j = 1, 2, 0$) generally take arbitrary functions of \hat{q}_\perp^2 and \hat{q}_0^2 . The most generic form of the potentials is given by rational functions of $z \equiv \hat{q}_0^2$,

$$y_j(\hat{q}) = \frac{P_j(z)}{Q_j(z)}, \quad (114)$$

where $Q_j(z) \geq 0$ in a range of $0 \leq z \leq 1$.

F. RG equations with approximations

To gain an insight from the functional RG equations, we solve the equations with two approximations. Firstly, we solve Eqs. (111,112,113) only at an equator of the unit sphere [$(|\hat{q}_\perp|, |\hat{q}_0|) = (1, 0)$] and at the poles of the sphere [$(|\hat{q}_\perp|, |\hat{q}_0|) = (0, 1)$], and interpolate intermediate values of $y_j(\hat{q})$ in terms of the following ansatzes;

$$y_1(\hat{q}) = \frac{A_1}{\hat{q}_\perp^2 + b_1 \hat{q}_0^2}, \quad y_2(\hat{q}) = \frac{A_2}{\hat{q}_\perp^2 + b_2 \hat{q}_0^2}, \quad (115)$$

$$y_0(\hat{q}) = \frac{A_0}{(\hat{q}_\perp^2 + b_0 \hat{q}_0^2)^2},$$

with $b_j \geq 0$ ($j = 1, 2, 0$). The values of $y_j(\hat{q})$ at the equator and poles for $j = 1, 2$ and those of $y_0(\hat{q})$ are represented by A_j and $B_j \equiv A_j/b_j$, and by A_0 and

$B_0 \equiv A_0/b_0^2$, respectively. The ansatzes give the following simple forms to the three types of the Coulomb interaction potentials in the coordinate space,

$$Y_1(r) = \frac{A_1}{\sqrt{b_1 r_\perp^2 + r_0^2}}, \quad Y_2(r) = \frac{A_2}{\sqrt{b_2 r_\perp^2 + r_0^2}}, \quad (116)$$

$$Y_0(r) = \frac{A_0}{2b_0} \begin{pmatrix} \sqrt{b_0} & & \\ & \sqrt{b_0} & \\ & & 1 \end{pmatrix} \eta_2 \frac{1 - \hat{r} \hat{r}^T}{|r|} \eta_2 \begin{pmatrix} \sqrt{b_0} & & \\ & \sqrt{b_0} & \\ & & 1 \end{pmatrix}, \quad (117)$$

with $r \equiv (\sqrt{b_0} r_\perp, r_0)$. Thereby, the three b_j parameters ($j = 1, 2, 0$) can be interpreted as effective metrics for each of the three potentials. Especially, the $Y_0(r)$ interaction in Eq. (117) can be considered as the dipolar interaction modulated by η_2 in the reframed coordinate [see Eq. (130)]. Eq. (116) also simplifies the second term of Eq. (110);

$$\frac{d\nu}{d \ln b} = 2\nu + 2\Delta \frac{\partial}{\partial \nu} \left(\frac{\sin \nu}{\nu} \right) A_+ = 2\nu \left(1 - \frac{\Delta}{3} (d_1 + d_2) A_+ \right), \quad (118)$$

with $A_+ \equiv A_1 + A_2$. Thanks to the approximation, Eqs. (111,112,113) reduce to RG equations among 6 coupling constants, A_j, B_j ($j = 1, 2, 0$). In terms of $A_+ \equiv A_1 + A_2$, $A_- \equiv A_1 - 2A_2$, $B_+ \equiv B_1 + B_2$, and $B_- \equiv B_1 - 2B_2$, they are particularly simplified,

$$\frac{dA_+}{d \ln b} = A_+ (1 - \Delta(d_1 - 2d_2)A_+), \quad (119)$$

$$\frac{dA_-}{d \ln b} = A_- (1 - \Delta(d_1 + d_2)A_-), \quad (120)$$

$$\frac{dB_+}{d \ln b} = B_+ (1 - \Delta(d_1 + d_2)B_+), \quad (121)$$

$$\frac{dB_-}{d \ln b} = B_- (1 - \Delta(d_1 + 4d_2)B_-), \quad (122)$$

$$\frac{dA_0}{d \ln b} = A_0 (1 - 2\Delta(d_1 + d_2)A_-) - \frac{\Delta}{9} (2(d_1 + d_2)A_+ A_- - (d_1 - 2d_2)A_+^2 - (d_1 + 4d_2)A_-^2), \quad (123)$$

$$\frac{dB_0}{d \ln b} = B_0 (1 - 2\Delta(d_1 + d_2)B_+) - \frac{\Delta}{9} (2(d_1 + d_2)B_+ B_- - (d_1 - 2d_2)B_+^2 - (d_1 + 4d_2)B_-^2). \quad (124)$$

Secondly, to evaluate the right-hand side of Eq. (109);

$$\frac{dx}{d \ln b} = x - 2 \left\{ \langle Y_1(\Omega) \rangle + \langle \Omega \cdot \eta_2 \cdot \Omega Y_2(\Omega) \rangle + \langle \Omega \cdot Y_0(\Omega) \cdot \Omega \rangle \right\}, \quad (125)$$

we take the statistical average with equal weight for Ω over the unit sphere S_2 ;

$$\begin{aligned} \langle Y(\Omega) \rangle &\equiv \frac{\int dl t^l \int D\Omega(\lambda) e^{-s_1(\Gamma)} f(\Omega(\lambda) a_0)}{\int dl t^l \int D\Omega(\lambda) e^{-s_1(\Gamma)}} \\ &= \frac{1}{4\pi} \int_{S_2} d^2\Omega Y(\Omega) + \mathcal{O}(\chi). \end{aligned} \quad (126)$$

Together with Eq. (115), this gives expressions for the right-hand side of Eq. (125);

$$\langle Y_1(\Omega) \rangle = \frac{A_1}{\sqrt{b_1 - 1}} \arcsin \left[\sqrt{\frac{b_1 - 1}{b_1}} \right], \quad (127)$$

$$\begin{aligned} \langle \Omega \cdot \eta_2 \cdot \Omega Y_2(\Omega) \rangle &= \\ \frac{A_2}{2(b_2 - 1)} \left(3 - \frac{2 + b_2}{\sqrt{b_2 - 1}} \arcsin \left[\sqrt{\frac{b_2 - 1}{b_2}} \right] \right), \end{aligned} \quad (128)$$

$$\begin{aligned} \langle \Omega \cdot Y_0(\Omega) \cdot \Omega \rangle &= \frac{9A_0}{4(b_0 - 1)^2} \left(-5 + 8\sqrt{b_0} \right. \\ &\quad \left. + \frac{2 - 5b_0}{\sqrt{b_0 - 1}} \arcsin \left[\sqrt{\frac{b_0 - 1}{b_0}} \right] \right), \end{aligned} \quad (129)$$

for $1 < b_i$. For $0 < b_i < 1$, $\frac{1}{\sqrt{b_i - 1}} \arcsin[\sqrt{1 - \frac{1}{b_i}}]$ is replaced by $\frac{1}{\sqrt{1 - b_i}} \operatorname{arcsinh}[\sqrt{\frac{1}{b_i} - 1}]$ [see also Appendix C].

G. phase diagram and emergent anisotropic correlations

The RG equations, Eqs. (118-129), are numerically solved for parameter regions of $x = a_0 \ln t$, $A_1 = B_1 \equiv y$, and $A_2 = B_2 = A_0 = B_0 = 0$ with $\nu = 0.1, 0.5$, and 1.0 [Fig.3]. A phase for a given set of parameters is determined by solutions of the differential equations in the infrared (IR) limit ($\ln b \rightarrow \infty$). To be specific, using the parameters as initial values of the differential equations, we solve the equations numerically, and see how the fugacity parameter $x = a_0 \ln t$ behaves in the IR limit. The phase diagram thus determined has a disorder phase with divergent t , and an ordered phase with vanishing t . The disordered phase is controlled by high- T fixed point with divergent t and vanishing ν . The high- T fixed point is isotropic both in space and vortex-vector space, i.e. $b_1 = b_2 = b_0 = 1$, and $A_2/A_1 = A_0/A_1 = 0$, where the dominant Coulomb interaction A_1 vanishes as $A_1 \simeq \frac{3}{2\pi^4} x e^{-\pi x}$. The disorder phase is essentially the same as the disorder phase without the 1D Berry phase term.

The ordered phase is controlled by low- T fixed region with divergent Berry phase parameter ν , vanishing t and divergent $A_1 (> 0)$. The low- T fixed region is generally anisotropic both in space and in vortex-vector space, where, in the IR limit, all of b_1 , b_2 , and b_0 converge to finite positive values greater than 1 [see Fig. 4(a,b)], and A_2/A_1 and A_0/A_1 approach finite positive and negative

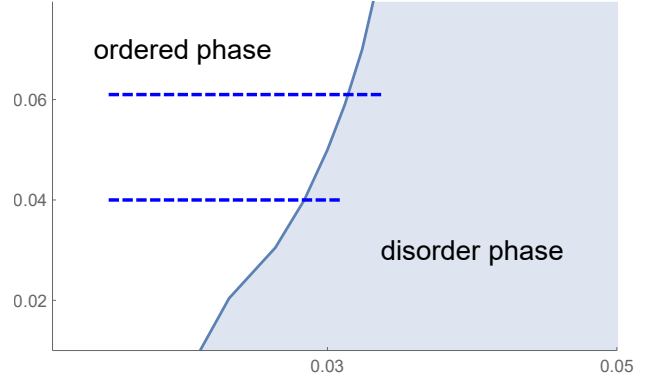


FIG. 3. An RG phase diagram of 3D Coulomb loop gas model with the 1D Berry phase term [$\nu = 0.5$]. The horizontal axis is the fugacity parameter [$\pi x \equiv \pi a_0 \ln t$], and vertical axis is $2\pi y \equiv 2\pi A_1 = 2\pi B_1$. Phases at a given (x, y) in the diagram is determined by behavior of the fugacity parameter in the infrared limit [$\ln b \rightarrow \infty$], when the RG equations, Eqs. (118-129), are numerically solved with the parameter $(A_1, B_1, a_0 \ln t, \nu) = (y, y, x, 0.5)$ as the initial parameters [$A_2 = B_2 = 0$ ($b_2 = 1$), $A_0 = B_0 = 0$ ($b_0 = 1$)]. In the ordered phase, $\ln t$ vanishes and A_j ($j = 1, 2, 0$) diverges in the IR limit, while in the disordered phase $\ln t$ diverges, and A_j ($j = 1, 2, 0$) vanishes in the IR limit. Along the blue dotted lines, Figs. 4 show how the renormalized values of b_j ($j = 1, 2, 0$) in the IR limit behave as a function of the initial value of x .

constants, respectively. $b_j > 1$ ($j = 1, 2, 0$) generally indicates that, by the renormalization effect, a characteristic length scale ξ_0 along the x_0 direction becomes longer than the length scale ξ_\perp within the x_1 - x_2 plane. As the characteristic length scale in the ordered phase is nothing but vortex-loop size, $b_j > 1$ means that the screening by shorter vortex loops elongates vortex loops along the x_0 direction. In fact, the Berry phase term suppresses the screening effect by unpolarized vortex loops, and the screening by polarized vortex loops tends to reduce the Coulomb interaction within the x_1 - x_2 plane more than it does along the x_0 direction. The spatial anisotropy in the Coulomb energy deforms a loop in such a way that the loop is effectively elongated along x_0 .

The F_2 interaction with the positive A_2 favors a parallel alignment of neighboring vortex segments along the x_0 direction, yielding a straight vortex line along x_0 . In fact, the screening by the polarized vortex loops tends to reduce the interaction between two vortex segments polarized along x_0 more than it does between two segments arranged otherwise. The $G(r)$ interaction with $b_0 \neq 1$ takes a form of the dipole-dipole interaction in a reframed coordinate, $\mathbf{x} \equiv (\sqrt{b_0} x_\perp, x_0)$,

$$\begin{aligned} \sum_{i,j} \oint_{\Gamma_i} \oint_{\Gamma_j} dx^i \cdot G(x-y) \cdot dy^j &= \frac{A_0}{2a_0 b_0} \sum_{i,j} \\ &\quad \oint_{\Gamma_i} \oint_{\Gamma_j} \frac{1}{|\mathbf{r}_{ij}|} dx^i \cdot \eta_2 \cdot (1 - \hat{r}_{ij} \hat{r}_{ij}^T) \cdot \eta_2 \cdot dy^j \end{aligned} \quad (130)$$

with $r_{ij} \equiv x^i - y^j$. The $G(r)$ interaction potential within a same loop ($i = j$) determines an energetics of the curved vortex loop in the reframed coordinate space. Especially, the G interaction with the negative A_0 favors a vortex loop curving within x_0 - x_1 or x_0 - x_2 planes over a loop curving within x_1 - x_2 plane. This helps the vortex loop to be confined within a plane parallel to the x_0 axis. With $b_0 > 1$, the polarized vortex loop is further elongated along the topological (x_0) direction in the original spatial coordinate.

Interestingly, the numerical solutions also find that near the boundary between ordered and disorder phases, b_j for all j diverge with essential singular forms (Fig. 4(a,b)). The divergence suggests that a ratio between ξ_0 and ξ_\perp diverges toward the boundary, $\xi_0/\xi_\perp \propto \exp[-c/|x - x_c|^\alpha]$. From the fitting of b_j for $j = 1, 2, 0$, α is estimated around $\alpha = 0.3 \sim 0.6$ (Fig. 4(c)). The differential equations have no saddle fixed point; a fixed point with the least number of relevant scaling variables turns out to have at least two relevant scaling variables. To deduce how ξ_\perp behaves near the ordered-disorder phase boundary, we regard that ξ_\perp at $|\ln t| = 1$ is on the order of the UV lattice constant a_0 , and solve the equations inversely up to parameters near the boundary. ξ_\perp thus determined has no divergence around the boundary (Fig. 4(a,b)).

V. DISCUSSION

In this paper, we have developed a perturbative renormalization group theory for 3D U(1) sigma model with 1D Berry phase term. An ordered-disorder transition of the U(1) sigma model is induced by the spatial proliferation of vortex loops. The 1D Berry phase term confers a complex phase factor upon those unpolarized vortex loops that have finite projections in a space complementary to a topological direction with the 1D Berry phase. The complex phase factor suppresses screening effects by the unpolarized vortex loops, while the screening by polarized vortex loops tends to confine other vortex loops to be within planes parallel to the topological direction. It also elongates the vortex loops along the topological direction. Numerical analyses of the approximated RG equations show that near a boundary between ordered and disorder phases, the length scale along the topological direction becomes anomalously larger, while the length scale within the other directions remains finite. Ultimately, the extreme spatial anisotropy of the vortex-loop length may lead to an emergence of a quasi-disorder phase between ordered and disorder phases. In the quasi-disorder phase, the correlation length along the topological direction is divergent, while it is finite along the others.

In fact, the emergence of the intermediate quasi-disorder phase is expected from a duality mapping between the U(1) sigma model with the 1D Berry phase and a lattice model of 3D type-II superconductor under an external magnetic field [7, 11, 30]. To see this mapping, let us first start from Eqs. (4.6) and explain how to reach a partition function of a cubic-lattice model of the type-II superconductors under the field,

$$\begin{aligned}
& 1 + \sum_{n=1}^{\infty} \frac{1}{n!} \prod_{j=1}^n \left(\int_{ab}^{\infty} \left(\frac{dl_j}{a_0} \right) t^{l_j} \int \left(\frac{d^3 R_j}{a_0^3} \right) \int D\Omega_j \right) \exp \left\{ \left[-2\pi i \int A(x) \cdot v(x) d^3x - 2\pi i \chi \sum_j S_{12}^j \right] \right\} \\
& \rightarrow \prod_{\mathbf{j}=(j_1, j_2, j_0)}^{j_1, j_2, j_0 \in \mathbf{Z}} \left(\int_0^{2\pi} \frac{d\phi_j}{2\pi} \right) \sum_{L=0}^{\infty} \frac{t^L}{L!} \left(\sum_{\mathbf{m}=(m_1, m_2, m_0)} \sum_{\sigma=\pm} \sum_{\nu=1,2,0} e^{i\sigma \left(\phi_{\mathbf{m}+\hat{\nu}} - \phi_{\mathbf{m}} + 2\pi A_{\mathbf{m},\nu} + \pi\chi(\delta_{\nu,1}m_2 - \delta_{\nu,2}m_1) \right)} \right)^L \\
& = \prod_{\mathbf{j}} \left(\int_0^{2\pi} \frac{d\phi_j}{2\pi} \right) \exp \left[2t \sum_{\mathbf{m}} \sum_{\nu} \cos \left(\phi_{\mathbf{m}+\hat{\nu}} - \phi_{\mathbf{m}} + 2\pi A_{\mathbf{m},\nu} + \pi\chi(\delta_{\nu,1}m_2 - \delta_{\nu,2}m_1) \right) \right]. \quad (131)
\end{aligned}$$

Here, \mathbf{j} , \mathbf{m} and $\mathbf{m} + \hat{\nu}$ ($\nu = 1, 2, 0$) in the right hand side are integer-valued 3D coordinates of dual cubic lattice sites, and $\hat{\nu}$ ($\nu = 1, 2, 0$) are the three orthogonal unit vectors. Real-valued $A_{\mathbf{m},\nu}$ stands for the vector potential in the lattice model, and $A_{\mathbf{m},\nu}$ lives on a link connecting \mathbf{m} and $\mathbf{m} + \hat{\nu}$. To describe the vortex vector field on the lattice, we introduce an integer-valued vector field $l_{\mathbf{m}} \equiv (l_{\mathbf{m},1}, l_{\mathbf{m},2}, l_{\mathbf{m},0})$ with $l_{\mathbf{m},\nu} \in \mathbf{Z}$. Namely,

we identify a surface integral of $v(x)$ over a $\mu\lambda$ -plaquette with $\epsilon_{\mu\lambda\nu} l_{\mathbf{m},\nu}$. Here the $\mu\lambda$ -plaquette stands for a unit plaquette of an original cubic lattice, subtended by the two orthogonal unit vectors, $\hat{\mu}$ and $\hat{\lambda}$, and the dual-cubic-lattice link at $(\mathbf{m}, \mathbf{m} + \hat{\nu})$ penetrates the plaquette. These translations allow us to rewrite $\int A(x) \cdot v(x) d^3x$ into $\sum_{\mathbf{m}} \sum_{\nu=1,2,0} A_{\mathbf{m},\nu} l_{\mathbf{m},\nu}$. As $\nabla \cdot v(x) = 0$, $l_{\mathbf{m}}$ also obeys a divergence-free condition on the lattice,

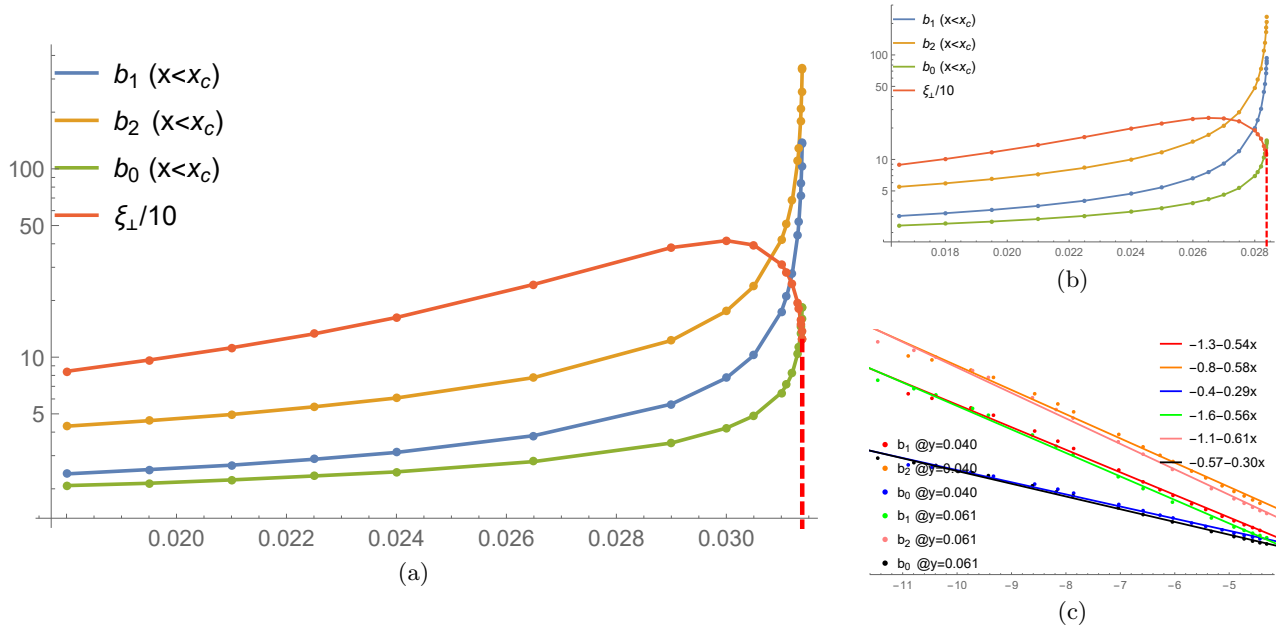


FIG. 4. (a,b) b_1 , b_2 , b_0 and ξ_{\perp} in the ordered phase near the order-disorder transition line at $\nu = 0.5$ and (a) $y = 0.061$, (b) $y = 0.040$. The horizontal axis is $x = a_0 \ln t$. The values of b_j and ξ_{\perp} at x in the figures are obtained from values of b_j and $\ln b$ at the low- T fixed region [$x = -1$], respectively, that is reached by numerical solutions of the differential equations with initial parameters (x, y, ν) , $A_2 = B_2 = A_0 = B_0 = 0$, $b_2 = b_0 = 1$ and $\ln b = 0$. (c) $\log b_j$ ($j = 1, 2, 0$) as a function of $\log|x - x_c|$ for $y = 0.040$ (red, orange, blue) and $y = 0.061$ (green, pink, black). Linear fitting curves is $\log b_j = c_0 + c_1 \log[|x - x_c|]$, where c_1 is around -0.3 for $j = 0$, and ranges from -0.5 to -0.6 for $j = 1, 2$.

$\sum_{\mu=1,2,0}(l_{\mathbf{m},\mu} - l_{\mathbf{m}-\hat{\mu},\mu}) = 0$. In the right hand side of the mapping, a sum over all possible configurations of $l_{\mathbf{m}}$ under the divergence-free condition is performed by multiple integral over $U(1)$ phase variables $\phi_{\mathbf{m}}$ on the dual cubic lattice sites. Thereby, $\sigma = \pm$ stands for ± 1 vorticity of the vortex segment on the link $(\mathbf{m}, \mathbf{m} + \hat{\nu})$, $\ln t$ stands for the chemical potential of the vortex loop with the unit vorticity per the unit cubic-lattice constant, and the integer L corresponds to a length of the closed vortex loop on the lattice.

A trivial addition of the Maxwell term Eq. (5) into the right hand side of Eq. (131) completes the duality mapping;

$$Z_{\nu} \rightarrow \int DA_{\mathbf{m}} \int D\phi_{\mathbf{m}} \exp \left[-\frac{T}{2} \sum_{\mathbf{m}} (\nabla \times A_{\mathbf{m}})^2 + 2t \sum_{\mathbf{m}} \sum_{\nu} \cos \left(\phi_{\mathbf{m}+\hat{\nu}} - \phi_{\mathbf{m}} + 2\pi A_{\mathbf{m},\nu} + \pi\chi(\delta_{\nu,1}m_2 - \delta_{\nu,2}m_1) \right) \right]. \quad (132)$$

The dual lattice model thus obtained portrays the magnetostatics of the type-II superconductor under an external magnetic field. In the dual model, $\phi_{\mathbf{m}}$ stands for a $U(1)$ phase of the superconducting order parameter on the dual lattice site \mathbf{m} , and the fugacity parameter t plays the role of the Josephson coupling between neighboring superconducting order parameters. Thereby, the

disorder phase with the divergent fugacity t in the sigma model maps into the superconducting (Meissner) phase, and the ordered phase with vanishing fugacity t is into the normal (Maxwell) phase in the dual model. Importantly, the 1D Berry phase term χ becomes an external magnetic field applied along the topological (x_0) direction in the dual lattice model.

It is well known that the type-II superconductors under the magnetic field along x_0 have intermediate mixed phase(s), where magnetic flux lines run along x_0 , and they are separated by a finite distance within x_1 - x_2 planes [10]. Thus, the mapping indicates that a similar intermediate phase must also appear between ordered and disorder phases in the $U(1)$ sigma model with the 1D Berry phase term, and the intermediate phase here is nothing but the quasi-disorder phase. In fact, the extremely spatially anisotropic correlation function expected in the quasi-disorder phase is consistent with the physical properties of the mixed phases in the type-II superconductors.

To see more clearly the correspondence between the quasi-disorder phase in the sigma model and the mixed phase in the type-II superconductor, let us start from the correlation function of $e^{i\theta(x)}$ in the sigma model, and disregard its spin-wave contribution. That is to say, the correlation function is solely given by a Dirac-string field

$h(x)$,

$$\begin{aligned} & \langle e^{-i(\theta(y)-\theta(z))} \rangle_{\text{NLSM}} \\ & \simeq \frac{1}{Z_V} \int D u_T \int D H e^{-\frac{T}{2} \int H^2 d^3 x - i \int H \cdot u_T d^3 x}, \end{aligned} \quad (133)$$

with $\nabla \cdot h(x) = \delta(x - y) - \delta(x - z)$, and $Z_V = \int D u_T \int D H e^{-\frac{T}{2} \int H^2 d^3 x - i \int H \cdot u_T d^3 x}$. The Dirac string field $h(x)$ is a magnetic flux that emanates from a pair of magnetic charges placed at the two test points, y and z . The Dirac string field yields an additional vector potential $a(x)$ in the left hand side of Eq. (131) as $A(x) \rightarrow A(x) + a(x)$ with $h(x) \equiv \nabla \times a(x)$. Thus, the duality transformation relates the correlation function with a ratio between partition functions of the lattice superconductor model with and without the magnetic charges [7, 30],

$$\langle e^{i\theta(y)-i\theta(z)} \rangle \rightarrow Z_{\text{LS}}[a]/Z_{\text{LS}}[a=0]. \quad (134)$$

Here $Z_{\text{LS}}[a]$ stands for the partition function with the magnetic charges,

$$\begin{aligned} Z_{\text{LS}}[a] \equiv & \int D A_{\mathbf{m}} \int D \phi_{\mathbf{m}} \exp \left[-\frac{T}{2} \sum_{\mathbf{m}} (\nabla \times A_{\mathbf{m}})^2 \right. \\ & + 2t \sum_{\mathbf{m}} \sum_{\nu} \cos \left(\phi_{\mathbf{m}+\hat{\nu}} - \phi_{\mathbf{m}} + 2\pi A_{\mathbf{m},\nu} \right. \\ & \left. \left. + 2\pi a_{\mathbf{m},\nu} + \pi \chi(\delta_{\nu,1} m_2 - \delta_{\nu,2} m_1) \right) \right]. \end{aligned} \quad (135)$$

In the right hand side, the rotation of $a_{\mathbf{m}}$ describes the Dirac string field in the dual lattice model. The Dirac string on the lattice can be depicted by a quantized flux line with an arrow that goes through cubic lattice sites from $\bar{\mathbf{n}}$ to $\bar{\mathbf{l}}$. Here, $\bar{\mathbf{n}}$ and $\bar{\mathbf{l}}$ denote the original cubic lattice sites that correspond to the two test points, y and z , respectively. Thereby, $(\nabla \times a_{\mathbf{m}})_{\nu} \equiv \epsilon_{\nu\lambda\mu} (a_{\mathbf{m},\lambda} - a_{\mathbf{m}+\hat{\nu},\lambda}) \equiv h_{\bar{\mathbf{m}},\nu}$ takes +1 and -1 when the original cubic lattice link $(\bar{\mathbf{m}}, \bar{\mathbf{m}} + \hat{\nu})$ is on the Dirac string line, and $\hat{\nu}$ is parallel and antiparallel to the arrow, respectively. Otherwise, the rotation takes 0.

In mixed phases with the magnetic flux lines along x_0 , the right-hand side of Eq. (134) remains finite for large $|y-z|$ in the parallel geometry [$y-z \parallel$ the x_0 axis], while it decays exponentially in the distance in the perpendicular geometry [$y-z \perp$ the x_0 axis]. Namely, $Z_{\text{LS}}[a]$ in the parallel geometry becomes independent from larger $|y-z|$, because the Dirac string field $h(x)$ emanating from the magnetic charges will be trapped by one of the magnetic flux lines near y and z , such that $h(x)$ inside the flux line will not feel the Meissner (Higgs) mass. In the perpendicular geometry, however, $Z_{\text{LS}}[a]$ decays exponentially in the larger distance $|y-z|$, because a superconducting region to which the Dirac string field is exposed is inevitably proportional to $|y-z|$. These considerations together with Eq. (134) suggest that the quasi-disorder

phase in the sigma model corresponds to the mixed phase in its dual model.

In conclusion, the mapping together with the vortex physics in type-II superconductors indicates the emergence of the intermediate quasi-disorder phase in the U(1) sigma model with 1D Berry phase term. In the intermediate phase, the exponential correlation length is divergent along the topological (x_0) direction with the 1D Berry phase, while it is finite along the others. Contrary to the argument in this section, the result in Section IVG fails to find a stable fixed point for the intermediate quasi-disorder phase. The failure may stem from one of the two approximations introduced in Section IVF, i.e. Eq. (126); the approximation has no ground to be justified.

ACKNOWLEDGMENTS

We thank Lingxian Kong, Yeyang Zhang, and Zhenyu Xiao for discussions. The work was supported by the National Basic Research Programs of China (No. 2019YFA0308401) and the National Natural Science Foundation of China (No. 11674011 and No. 12074008).

Appendix A: Linear confining potential between monopole and antimonopole

In the main text, we considered only vortex loops, while one could also consider a vortex line with open ends. In this appendix, we show that the two endpoints attract each other by a linear confining potential [7, 30].

In the presence of the open ends, the divergence of the vortex vector is no longer zero, and it gives two point charges that can be regarded as magnetic monopole and anti-monopole,

$$\begin{aligned} \nabla \cdot v(x) &= \int_{x^j(0)=x_{\text{mm}}}^{x^j(l^j)=x_{\text{am}}} dx^j \cdot \nabla \delta(x - x^j) \\ &= \delta(x - x_{\text{mm}}) - \delta(x - x_{\text{am}}). \end{aligned} \quad (A1)$$

Here two ends are at $x = x_{\text{mm}}$ and $x = x_{\text{am}}$, and vorticity is from $x = x_{\text{mm}}$ to $x = x_{\text{am}}$. An interaction between the two point charges is encoded in the second term of Eq. (8);

$$\begin{aligned} & -\frac{4\pi^2}{2T} \int_{k \neq 0} \frac{dk^3}{(2\pi)^3} \frac{1}{k^4} (\nabla \cdot v)_k (\nabla \cdot v)_{-k} \\ & \equiv -\frac{1}{2T} \int d^3 x \int d^3 y V(x-y) (\nabla \cdot v(x)) (\nabla \cdot v(y)). \end{aligned} \quad (A2)$$

The interaction potential thus introduced is attractive

and linear in the distance between the charges;

$$\begin{aligned}
V(r) &= \int_{k \neq 0} \frac{d^3 k}{(2\pi)^3} \frac{4\pi^2}{k^4} e^{ikr} = \frac{1}{i|r|} \int_{\varepsilon}^{\infty} dk \frac{e^{ik|r|} - e^{-ik|r|}}{k^3} \\
&= -\frac{1}{i|r|} \left[\frac{1}{\varepsilon^2} \int_{\pi}^0 id\theta e^{-2i\theta} + \frac{i|r|}{\varepsilon} \int_{\pi}^0 id\theta e^{-i\theta} \right. \\
&\quad \left. - \frac{1}{2}|r|^2 \int_{\pi}^0 id\theta + \mathcal{O}(\varepsilon) \right] \\
&= \frac{2}{\varepsilon} - \frac{\pi}{2}|r| + \mathcal{O}(\varepsilon). \tag{A3}
\end{aligned}$$

Here, ε is an infinitesimally small positive quantity associated with the principal-value integral in the first line. Since $\int \nabla \cdot v(x) dx = 0$, the first term in the last line of Eq. (A3) vanishes when substituted into Eq. (A2), and we obtain the linear confining potential between magnetic monopole and anti-monopole;

$$S_0 = \dots - \frac{\pi}{2T} |x_{\text{am}} - r_{\text{mm}}|. \tag{A4}$$

A second-order spatial derivative of the linear confining potential yields a dipole-dipole interaction between magnetic dipoles at x_{am} and x_{mm} ,

$$-\frac{\partial S_0}{\partial x_{\text{am},\mu} \partial x_{\text{mm},\nu}} = \frac{\pi}{2T} \left(\frac{1 - \hat{r}\hat{r}^T}{|r|} \right), \tag{A5}$$

with $r \equiv x_{\text{am}} - r_{\text{mm}}$.

Appendix B: renormalization to the anisotropic Coulomb potentials

In Section IV, several terms in $2(\sum_j s_0(\Gamma, \Gamma_j))^2$ have been calculated. In this appendix, the rest will be calculated. A coupling between $\nabla_{R_\lambda} F_2(R - x^i)$ and $\nabla_{R_\rho} F_2(R - y^j)$ in $2(\sum_j s_0(\Gamma, \Gamma_j))^2$ is given by

$$\begin{aligned}
&\sum_{i=1}^n \sum_{j=1}^n \oint_{\Gamma_i} dx_\phi^i(\eta_2)_{\phi\phi} \oint_{\Gamma_j} dy_\sigma^j(\eta_2)_{\sigma\sigma} \int_V d^3 R \int_{S_2} d^2 \Omega e^{-i\nu \cos \theta} \\
&\frac{a_0^4 \pi^2}{8} \Omega_\mu \Omega_\psi \epsilon_{\mu\lambda\phi} \epsilon_{\psi\rho\sigma} \left(\nabla_{R_\lambda} F_2(R - x^i) \right) \left(\nabla_{R_\rho} F_2(R - y^j) \right) \\
&= \frac{a_0^4 \pi^3}{6} \sum_{i,j} \epsilon_{\mu\lambda\phi} \epsilon_{\mu\rho\sigma} (d_1 \delta_{\mu\mu} + d_2 (\eta_2)_{\mu\mu}) \\
&\quad \int_V d^3 R \oint_{\Gamma_i} dx_\phi^i(\eta_2)_{\phi\phi} \oint_{\Gamma_j} dy_\sigma^j(\eta_2)_{\sigma\sigma} \\
&\quad \left(\nabla_{R_\lambda} F_2(R - x^i) \right) \left(\nabla_{R_\rho} F_2(R - y^j) \right). \tag{B1}
\end{aligned}$$

A multiplication of the second line of Eq. (74) by $(\eta_2)_{\phi\phi}$ and $(\eta_2)_{\sigma\sigma}$ facilitates a subsequent calculation of

Eq. (B1) ;

$$\begin{aligned}
&\epsilon_{\mu\lambda\phi} \epsilon_{\mu\rho\sigma} (d_1 \delta_{\mu\mu} + d_2 (\eta_2)_{\mu\mu}) (\eta_2)_{\phi\phi} (\eta_2)_{\sigma\sigma} \\
&= d_1 (\delta_{\lambda\rho} (\eta_2^2)_{\phi\sigma} - (\eta_2)_{\lambda\sigma} (\eta_2)_{\phi\rho}) \\
&\quad + d_2 (- (\eta_2)_{\lambda\rho} (\eta_2^2)_{\phi\sigma} - \delta_{\lambda\rho} (\eta_2^3)_{\phi\sigma} \\
&\quad \quad + (\eta_2^2)_{\lambda\sigma} (\eta_2)_{\phi\rho} + (\eta_2)_{\lambda\sigma} (\eta_2^2)_{\phi\rho}) \\
&= 2(d_1 + d_2) \delta_{\lambda\rho} \delta_{\phi\sigma} - (d_1 + 3d_2) \delta_{\lambda\rho} (\eta_2)_{\phi\sigma} \\
&\quad - 2d_2 ((\eta_2)_{\lambda\rho} \delta_{\phi\sigma} - (\eta_2)_{\lambda\sigma} \delta_{\phi\rho} - \delta_{\lambda\sigma} (\eta_2)_{\phi\rho}) \\
&\quad + d_2 (\eta_2)_{\lambda\rho} (\eta_2)_{\phi\sigma} - (d_1 + 2d_2) (\eta_2)_{\lambda\sigma} (\eta_2)_{\phi\rho}, \tag{B2}
\end{aligned}$$

with $\eta_2^2 = -\eta_2 + 2$, and $\eta_2^3 = 3\eta_2 - 2$. Dropping terms with a factor of either $\delta_{\lambda\sigma}$ or $\delta_{\phi\rho}$, we obtain

$$\begin{aligned}
&\sum_{i=1}^n \sum_{j=1}^n \oint_{\Gamma_i} dx_\phi^i(\eta_2)_{\phi\phi} \oint_{\Gamma_j} dy_\sigma^j(\eta_2)_{\sigma\sigma} \int_V d^3 R \int_{S_2} d^2 \Omega e^{-i\nu \cos \theta} \\
&\quad \frac{a_0^4 \pi^2}{8} \Omega_\mu \Omega_\psi \epsilon_{\mu\lambda\phi} \epsilon_{\psi\rho\sigma} \left(\nabla_{R_\lambda} F_2(R - x^i) \right) \left(\nabla_{R_\rho} F_2(R - y^j) \right) \\
&= \sum_{i,j} \oint_{\Gamma_i} \oint_{\Gamma_j} \left(dx^i \cdot dy^j c_{221}(x^i - y^j) \right. \\
&\quad \quad + dx^i \cdot \eta_2 \cdot dy^j c_{222}(x^i - y^j) \\
&\quad \quad \left. + dx^i \cdot c_{220}(x^i - y^j) \cdot dy^j \right), \tag{B3}
\end{aligned}$$

with

$$\begin{aligned}
c_{221}(x^i - y^j) &\equiv \frac{a_0^4 \pi^3}{6} \left(2(d_1 + d_2) \delta_{\lambda\lambda} - 2d_2 (\eta_2)_{\lambda\lambda} \right) \\
&\quad \int_V d^3 R \left(\nabla_{R_\lambda} F_2(R - x^i) \right) \left(\nabla_{R_\lambda} F_2(R - y^j) \right), \tag{B4} \\
c_{222}(x^i - y^j) &\equiv \frac{a_0^4 \pi^3}{6} \left(- (d_1 + 3d_2) \delta_{\lambda\lambda} + d_2 (\eta_2)_{\lambda\lambda} \right) \\
&\quad \int_V d^3 R \left(\nabla_{R_\lambda} F_2(R - x^i) \right) \left(\nabla_{R_\lambda} F_2(R - y^j) \right), \tag{B5} \\
(c_{220})_{\phi\sigma}(x^i - y^j) &\equiv \frac{a_0^4 \pi^3}{6} (-) (d_1 + 2d_2) (\eta_2)_{\phi\rho} (\eta_2)_{\lambda\sigma} \\
&\quad \int_V d^3 R \left(\nabla_{R_\lambda} F_2(R - x^i) \right) \left(\nabla_{R_\rho} F_2(R - y^j) \right). \tag{B6}
\end{aligned}$$

Their Fourier transforms can be included into renormalization of $F_1(q)$, $F_2(q)$ and $G_0(q)$;

$$c_{221}(q) = \frac{a_0^4 \pi^3}{6} \left(2d_1 q^2 + 6d_2 q_0^2 \right) F_2^2(q), \tag{B7}$$

$$c_{222}(q) = \frac{a_0^4 \pi^3}{6} \left(- (d_1 + 3d_2) q^2 + d_2 (\eta_2)_{\lambda\lambda} q_\lambda^2 \right) F_2^2(q), \tag{B8}$$

$$c_{220}(q) \equiv \frac{a_0^4 \pi^3}{6} (-) (d_1 + 2d_2) q^2 F_2^2(q). \tag{B9}$$

with $(c_{220})_{\phi\sigma}(q) \equiv c_{220}(q) (\eta_2 \hat{q} \hat{q}^T \eta_2)_{\phi\sigma}$.

A coupling between $\nabla_{R_\lambda} F_1(R - x^i)$ and $\nabla_{R_\rho} G(R - y^j)$

in $2(\sum_j s_0(\Gamma, \Gamma_j))^2$ is summarized as follows

$$\begin{aligned}
& \sum_{i=1}^n \sum_{j=1}^n \oint_{\Gamma_i} dx_\phi^i \oint_{\Gamma_j} dy_\gamma^j \int_V d^3 R \int_{S_2} d^2 \Omega e^{-i\nu \cos \theta} \frac{a_0^4 \pi^2}{4} \\
& \Omega_\mu \Omega_\psi \epsilon_{\mu\lambda\phi} \epsilon_{\psi\rho\sigma} \left(\nabla_{R_\lambda} F_1(R-x^i) \right) \left(\nabla_{R_\rho} G_{\sigma\gamma}(R-y^j) \right) \\
& = \frac{a_0^4 \pi^3}{3} \sum_{i,j} \epsilon_{\mu\lambda\phi} \epsilon_{\mu\rho\sigma} (d_1 \delta_{\mu\mu} + d_2 (\eta_2)_{\mu\mu}) \int_V d^3 R \\
& \oint_{\Gamma_i} dx_\phi^i \oint_{\Gamma_j} dy_\gamma^j \left(\nabla_{R_\lambda} F_1(R-x^i) \right) \left(\nabla_{R_\rho} G_{\sigma\gamma}(R-y^j) \right) \\
& \equiv \sum_{i,j} \oint_{\Gamma_i} \oint_{\Gamma_j} dx^i \cdot c_{100}(x^i - y^j) \cdot dy^j. \quad (\text{B10})
\end{aligned}$$

3 by 3 $c_{100}(x^i - y^j)$ can be included as renormalization to $G(x^i - y^j)$ in $\bar{s}_0(\Gamma_i, \Gamma_j)$ of Eq. (73). One can see this, from the Fourier transform of $c_{110}(x^i - y^j)$;

$$\begin{aligned}
& (c_{100})_{\phi\gamma}(q) \\
& = \frac{a_0^4 \pi^3}{3} \epsilon_{\mu\lambda\phi} \epsilon_{\mu\rho\sigma} (d_1 \delta_{\mu\mu} + d_2 (\eta_2)_{\mu\mu}) \\
& \quad q_\lambda q_\rho F_1(q) G_0(q) (\eta_2)_{\sigma\sigma} \hat{q}_\sigma \hat{q}_\gamma (\eta_2)_{\gamma\gamma}, \\
& = \frac{a_0^4 \pi^3}{3} \left(-2d_2 (\delta_{\lambda\rho} \delta_{\phi\sigma} - \delta_{\lambda\sigma} \delta_{\phi\rho}) \right. \\
& \quad + (d_1 + d_2) (\delta_{\lambda\rho} (\eta_2)_{\phi\sigma} - (\eta_2)_{\lambda\sigma} \delta_{\phi\rho}) \\
& \quad \left. + d_2 (-(\eta_2)_{\lambda\rho} (\eta_2)_{\phi\sigma} + (\eta_2)_{\lambda\sigma} (\eta_2)_{\phi\rho}) \right) \\
& \quad q_\lambda q_\rho \hat{q}_\sigma F_1(q) G_0(q) \hat{q}_\gamma (\eta_2)_{\gamma\gamma}, \\
& \equiv c_{100}(q) (\eta_2)_{\phi\sigma} \hat{q}_\sigma \hat{q}_\gamma (\eta_2)_{\gamma\gamma},
\end{aligned}$$

with

$$c_{100}(q) = \frac{a_0^4 \pi^3}{3} (d_1 + d_2) q^2 F_1(q) G_0(q). \quad (\text{B11})$$

In the second line, we use Eq. (88). From the second line to the third line, we drop terms with $\delta_{\phi\lambda}$, $\delta_{\phi\rho}$ or $\delta_{\phi\sigma}$, by the integration by parts. By the re-exponentiation, Eq. (B11) produces the renormalization of $G_0(q)$ in $\bar{s}_0(\Gamma_i, \Gamma_j)$ s in Eq. (73).

A coupling between $\nabla_{R_\lambda} F_2(R-x^i)$ and $\nabla_{R_\rho} G(R-y^j)$ in $2(\sum_j s_0(\Gamma, \Gamma_j))^2$ is summarized by

$$\begin{aligned}
& \sum_{i=1}^n \sum_{j=1}^n \oint_{\Gamma_i} dx_\phi^i (\eta_2)_{\phi\phi} \oint_{\Gamma_j} dy_\gamma^j \int_V d^3 R \int_{S_2} d^2 \Omega e^{-i\nu \cos \theta} \\
& \frac{a_0^4 \pi^2}{4} \Omega_\mu \Omega_\psi \epsilon_{\mu\lambda\phi} \epsilon_{\psi\rho\sigma} \left(\nabla_{R_\lambda} F_2(R-x^i) \right) \left(\nabla_{R_\rho} G_{\sigma\gamma}(R-y^j) \right) \\
& = \frac{a_0^4 \pi^3}{3} \sum_{i,j} \epsilon_{\mu\lambda\phi} \epsilon_{\mu\rho\sigma} (d_1 \delta_{\mu\mu} + d_2 (\eta_2)_{\mu\mu}) \\
& \quad \int_V d^3 R \oint_{\Gamma_i} dx_\phi^i (\eta_2)_{\phi\phi} \oint_{\Gamma_j} dy_\gamma^j \\
& \quad \left(\nabla_{R_\lambda} F_2(R-x^i) \right) \left(\nabla_{R_\rho} G_{\sigma\gamma}(R-y^j) \right) \\
& \equiv \sum_{i,j} \oint_{\Gamma_i} \oint_{\Gamma_j} dx^i \cdot c_{200}(x^i - y^j) \cdot dy^j. \quad (\text{B12})
\end{aligned}$$

The Fourier-transform $c_{200}(q)$ of the 3 by 3 $c_{200}(x^i - y^j)$ yields the renormalization to $G_0(q)$ in $\bar{s}_0(\Gamma_i, \Gamma_j)$ s in Eq. (73);

$$\begin{aligned}
& (c_{200})_{\phi\gamma}(q) = \frac{a_0^4 \pi^3}{3} \epsilon_{\mu\lambda\phi} \epsilon_{\mu\rho\sigma} (d_1 \delta_{\mu\mu} + d_2 (\eta_2)_{\mu\mu}) (\eta_2)_{\phi\phi} q_\lambda q_\rho F_2(q) G_0(q) (\eta_2)_{\sigma\sigma} \hat{q}_\sigma \hat{q}_\gamma (\eta_2)_{\gamma\gamma} \\
& = \frac{a_0^4 \pi^3}{3} \left(2(d_1 + d_2) \delta_{\lambda\rho} \delta_{\phi\sigma} - (d_1 + 3d_2) \delta_{\lambda\rho} (\eta_2)_{\phi\sigma} - 2d_2 ((\eta_2)_{\lambda\rho} \delta_{\phi\sigma} \right. \\
& \quad \left. - (\eta_2)_{\lambda\sigma} \delta_{\phi\rho} - \delta_{\lambda\sigma} (\eta_2)_{\phi\rho}) + d_2 (\eta_2)_{\lambda\rho} (\eta_2)_{\phi\sigma} - (d_1 + 2d_2) (\eta_2)_{\lambda\sigma} (\eta_2)_{\phi\rho} \right) q_\lambda q_\rho \hat{q}_\sigma F_2(q) G_0(q) \hat{q}_\gamma (\eta_2)_{\gamma\gamma} \\
& = c_{200}(q) (\eta_2)_{\phi\sigma} \hat{q}_\sigma \hat{q}_\gamma (\eta_2)_{\gamma\gamma},
\end{aligned}$$

with

$$c_{200}(q) = \frac{a_0^4 \pi^3}{3} (-)(d_1 + d_2) (q^2 + (\eta_2)_{\lambda\lambda} q_\lambda^2) F_2(q) G_0(q). \quad (\text{B13})$$

Here we use Eq. (B2), and drop terms with factors of $\delta_{\phi\lambda}$, $\delta_{\phi\rho}$ or $\delta_{\phi\sigma}$ through the integration by parts.

A coupling between $\nabla_{R_\lambda} G(R-x^i)$ and $\nabla_{R_\rho} G(R-y^j)$ in $2(\sum_j s_0(\Gamma, \Gamma_j))^2$ is given by

$$\begin{aligned}
& \sum_{i=1}^n \sum_{j=1}^n \oint_{\Gamma_i} dx_\kappa^i \oint_{\Gamma_j} dy_\gamma^j \int_V d^3 R \int_{S_2} d^2 \Omega e^{-i\nu \cos \theta} \frac{a_0^4 \pi^2}{8} \Omega_\mu \Omega_\psi \epsilon_{\mu\lambda\phi} \epsilon_{\psi\rho\sigma} \left(\nabla_{R_\lambda} G_{\phi\kappa}(R-x^i) \right) \left(\nabla_{R_\rho} G_{\sigma\gamma}(R-y^j) \right) \\
& = \frac{a_0^4 \pi^3}{6} \sum_{i,j} \epsilon_{\mu\lambda\phi} \epsilon_{\mu\rho\sigma} (d_1 \delta_{\mu\mu} + d_2 (\eta_2)_{\mu\mu}) \int_V d^3 R \oint_{\Gamma_i} dx_\kappa^i \oint_{\Gamma_j} dy_\gamma^j \left(\nabla_{R_\lambda} G_{\phi\kappa}(R-x^i) \right) \left(\nabla_{R_\rho} G_{\sigma\gamma}(R-y^j) \right) \\
& \equiv \sum_{i,j} \oint_{\Gamma_i} \oint_{\Gamma_j} dx^i \cdot c_{000}(x^i - y^j) \cdot dy^j. \quad (\text{B14})
\end{aligned}$$

The Fourier transform of $c_{000}(x^i - y^j)$ is calculated as follows,

$$\begin{aligned}
(c_{000})_{\kappa\gamma}(q) &= \frac{a_0^4 \pi^3}{6} \epsilon_{\mu\lambda\phi} \epsilon_{\mu\rho\sigma} (d_1 \delta_{\mu\mu} + d_2 (\eta_2)_{\mu\mu}) q_\lambda q_\rho G_0(q) G_0(q) (\eta_2)_{\phi\phi} \hat{q}_\phi \hat{q}_\kappa (\eta_2)_{\kappa\kappa} (\eta_2)_{\sigma\sigma} \hat{q}_\sigma \hat{q}_\gamma (\eta_2)_{\gamma\gamma} \\
&= \frac{a_0^4 \pi^3}{6} \left(2(d_1 + d_2) \delta_{\lambda\rho} \delta_{\phi\sigma} - (d_1 + 3d_2) \delta_{\lambda\rho} (\eta_2)_{\phi\sigma} - 2d_2 ((\eta_2)_{\lambda\rho} \delta_{\phi\sigma} - (\eta_2)_{\lambda\sigma} \delta_{\phi\rho} - \delta_{\lambda\sigma} (\eta_2)_{\phi\rho}) \right. \\
&\quad \left. + d_2 (\eta_2)_{\lambda\rho} (\eta_2)_{\phi\sigma} - (d_1 + 2d_2) (\eta_2)_{\lambda\sigma} (\eta_2)_{\phi\rho} \right) q_\lambda q_\rho \hat{q}_\phi \hat{q}_\sigma G_0(q) G_0(q) \hat{q}_\kappa (\eta_2)_{\kappa\kappa} \hat{q}_\gamma (\eta_2)_{\gamma\gamma} \\
&= c_{000}(q) (\eta_2)_{\kappa\kappa} \hat{q}_\kappa \hat{q}_\gamma (\eta_2)_{\gamma\gamma},
\end{aligned}$$

with

$$c_{000}(q) = \frac{a_0^4 \pi^3}{6} (d_1 + d_2) q^2 \left(2 - (\eta_2)_{\lambda\lambda} \hat{q}_\lambda^2 - ((\eta_2)_{\lambda\lambda} \hat{q}_\lambda^2)^2 \right) G_0(q) G_0(q). \quad (\text{B15})$$

Appendix C: Integrals of Eq. (129)

Here we outline an integral calculation of Eq. (129) as a memorandum;

$$\langle \Omega \cdot Y_0(\Omega) \cdot \Omega \rangle = \int_{S_2} d^2\Omega \int \frac{d^3q}{(2\pi)^3} e^{iq\Omega - \alpha|q|} \frac{1}{q^2} \frac{A_0}{(\hat{q}_\perp^2 + b_0 \hat{q}_0^2)^2} (\Omega \cdot \eta_2 \cdot \hat{q})^2. \quad (\text{C1})$$

An infinitesimally small and positive α in the right-hand side controls the q -integral in the UV regime. The convergence factor is taken to zero in the end. With $\Omega \equiv (\sin \varphi \cos \psi, \sin \varphi \sin \psi, \cos \varphi)$, $q \equiv |q|(\sin \theta \cos \phi, \sin \theta \sin \phi, \cos \theta) \equiv |q|\hat{q}$, integrals over $|q|$ and $\psi - \phi$ yield,

$$\begin{aligned}
\langle \Omega \cdot Y_0(\Omega) \cdot \Omega \rangle &= -\frac{A_0}{(2\pi)^2} \int_{-1}^1 d(\cos \varphi) \int_{-1}^1 d(\cos \theta) \frac{1}{(\sin^2 \theta + b_0 \cos^2 \theta)^2} \\
&\quad \times \int_0^{2\pi} d\phi \frac{4 \cos^2 \theta \cos^2 \varphi - 4 \cos \theta \sin \theta \cos \varphi \sin \varphi \cos \phi + \sin^2 \theta \sin^2 \varphi \cos^2 \phi}{i(\cos \theta \cos \varphi + \sin \theta \sin \varphi \cos \phi) - \alpha}. \quad (\text{C2})
\end{aligned}$$

The right-hand side after the θ -integral is an even function in $t \equiv \cos \varphi$. Thus, we consider only $0 < t < 1$ ($0 < \varphi < \frac{\pi}{2}$). For the last term in the integrand, we integrate over ϕ first and then over θ ,

$$\begin{aligned}
&\lim_{\alpha \rightarrow +0} \int_{-1}^1 d(\cos \theta) \frac{1}{(\sin^2 \theta + b_0 \cos^2 \theta)^2} \int_0^{2\pi} d\phi \frac{\sin^2 \theta \sin^2 \varphi \cos^2 \phi}{i(\cos \theta \cos \varphi + \sin \theta \sin \varphi \cos \phi) - \alpha} \\
&= \lim_{\alpha \rightarrow +0} \frac{\sin \varphi}{2i} \int_{-\infty}^{+\infty} ds \frac{1}{(1 + b_0 s^2)^2} \oint \frac{dz}{i} \frac{z^2 + z^{-2} + 2}{z^2 + 2(X + iY)z + 1} \\
&= -\frac{4\pi \sin^2 \varphi}{\cos \varphi} \int_0^1 dX \frac{1}{(1 + b_0 \tan^2 \varphi X^2)^2} \frac{X^2}{\sqrt{1 - X^2}} = -\pi^2 \frac{\sin^2 \varphi}{\cos \varphi} \frac{1}{\sqrt{(1 + b_0 \tan^2 \varphi)^3}}, \quad (\text{C3})
\end{aligned}$$

with $s \equiv \cot \theta$, $z \equiv e^{i\phi}$, $X \equiv s \cot \varphi$, $Y \equiv \alpha(\sqrt{1 + s^2}/\sin \varphi)$. In the z -integral along the unit circle in the second line, the pole at $z = 0$ does not contribute to the integral, while poles at $z = z_\pm \equiv -(X + iY) \pm \sqrt{|W|} e^{\frac{i}{2} \arg W}$ contribute to the integral for $0 < s < \tan \varphi$ and for $-\tan \varphi < s < 0$, respectively. Here $W \equiv (X + iY)^2 - 1 \simeq X^2 - 1 + 2iXY$. We take the same integrals for the other two in a similar way;

$$\begin{aligned}
&\lim_{\alpha \rightarrow +0} \int_{-1}^1 d(\cos \theta) \frac{1}{\sin^2 \theta + b_0 \cos^2 \theta} \int_0^{2\pi} d\phi \frac{4 \cos^2 \theta \cos^2 \varphi - 4 \cos \theta \sin \theta \cos \varphi \sin \varphi \cos \phi}{i(\cos \theta \cos \varphi + \sin \theta \sin \varphi \cos \phi) - \alpha} \\
&= -8\pi^2 \frac{\sin^2 \varphi}{\cos \varphi} \frac{1}{\sqrt{(1 + b_0 \tan^2 \varphi)^3}} \quad (\text{C4})
\end{aligned}$$

Finally, we take an integral over $t = \cos \varphi$, and obtain,

$$\begin{aligned}
\langle \Omega \cdot Y_0(\Omega) \cdot \Omega \rangle &= \frac{9A_0}{4} \int_0^1 dt \frac{t^2(1 - t^2)}{\sqrt{(b_0 - (b_0 - 1)t^2)^3}} \\
&= \begin{cases} \frac{9A_0}{4(b_0 - 1)^2} \left(-5 + 8\sqrt{b_0} + \frac{2-5b_0}{\sqrt{1-b_0}} \text{ArcSinh} \left[\sqrt{\frac{1-b_0}{b_0}} \right] \right) & 0 < b_0 < 1, \\ \frac{9A_0}{4(b_0 - 1)^2} \left(-5 + 8\sqrt{b_0} + \frac{2-5b_0}{\sqrt{-1+b_0}} \text{ArcSin} \left[\sqrt{\frac{b_0-1}{b_0}} \right] \right) & 1 < b_0. \end{cases} \quad (\text{C5})
\end{aligned}$$

- [1] V. N. Popov, Quantum vortices and phase transitions in bose systems, *Soviet Physics – JETP* **37**, 341 (1973).
- [2] F. Wiegel, Vortex-ring model of bose condensation, *Physica* **65**, 321 (1973).
- [3] T. Banks, R. Myerson, and J. Kogut, Phase transitions in abelian lattice gauge theories, *Nuclear Physics B* **129**, 493 (1977).
- [4] D. R. Nelson and J. Toner, Bond-orientational order, dislocation loops, and melting of solids and smectic-*a* liquid crystals, *Phys. Rev. B* **24**, 363 (1981).
- [5] G. A. Williams, Vortex-ring model of the superfluid λ transition, *Phys. Rev. Lett.* **59**, 1926 (1987).
- [6] M. B. Einhorn and R. Savit, Topological excitations in the abelian higgs model, *Phys. Rev. D* **17**, 2583 (1978).
- [7] M. E. Peskin, Mandelstam-'t hooft duality in abelian lattice models, *Annals of Physics* **113**, 122 (1978).
- [8] R. Savit, Duality in field theory and statistical systems, *Rev. Mod. Phys.* **52**, 453 (1980).
- [9] C. Dasgupta and B. I. Halperin, Phase transition in a lattice model of superconductivity, *Phys. Rev. Lett.* **47**, 1556 (1981).
- [10] G. Blatter, M. V. Feigel'man, V. B. Geshkenbein, A. I. Larkin, and V. M. Vinokur, Vortices in high-temperature superconductors, *Rev. Mod. Phys.* **66**, 1125 (1994).
- [11] A. K. Nguyen and A. Sudbø, Topological phase fluctuations, amplitude fluctuations, and criticality in extreme type-ii superconductors, *Phys. Rev. B* **60**, 15307 (1999).
- [12] A. K. Nguyen and A. Sudbø, Onsager loop transition and first-order flux-line lattice melting in high- T_c superconductors, *Phys. Rev. B* **57**, 3123 (1998).
- [13] A. K. Nguyen and A. Sudbø, Phase coherence and the boson analogy of vortex liquids, *Phys. Rev. B* **58**, 2802 (1998).
- [14] S. Ryu and D. Stroud, Nature of the low-field transition in the mixed state of high-temperature superconductors, *Phys. Rev. B* **57**, 14476 (1998).
- [15] R. Gade, Anderson localization for sublattice models, *Nuclear Physics B* **398**, 499 (1993).
- [16] R. Gade and F. Wegner, The $n = 0$ replica limit of $U(n)$ and $U(n)SO(n)$ models, *Nuclear Physics B* **360**, 213 (1991).
- [17] E. J. König, P. M. Ostrovsky, I. V. Protopopov, and A. D. Mirlin, Metal-insulator transition in two-dimensional random fermion systems of chiral symmetry classes, *Physical Review B* **85**, 195130 (2012).
- [18] A. Altland and R. Merkt, Spectral and transport properties of quantum wires with bond disorder, *Nuclear Physics B* **607**, 511 (2001).
- [19] A. Altland, D. Bagrets, L. Fritz, A. Kamenev, and H. Schmiedt, Quantum Criticality of Quasi-One-Dimensional Topological Anderson Insulators, *Physical Review Letters* **112**, 206602 (2014).
- [20] A. Altland, D. Bagrets, and A. Kamenev, Topology versus Anderson localization: Nonperturbative solutions in one dimension, *Physical Review B* **91**, 085429 (2015).
- [21] X. Luo, B. Xu, T. Ohtsuki, and R. Shindou, Critical behavior of Anderson transitions in three-dimensional orthogonal classes with particle-hole symmetries, *Physical Review B* **101**, 020202 (2020).
- [22] T. Wang, T. Ohtsuki, and R. Shindou, Universality classes of the anderson transition in the three-dimensional symmetry classes aiii, bdi, c, d, and ci, *Phys. Rev. B* **104**, 014206 (2021).
- [23] X. Luo, Z. Xiao, K. Kawabata, T. Ohtsuki, and R. Shindou, Unifying the Anderson transitions in Hermitian and non-Hermitian systems, *Physical Review Research* **4**, L022035 (2022).
- [24] J. F. Karcher, I. A. Gruzberg, and A. D. Mirlin, Metal-insulator transition in a two-dimensional system of chiral unitary class, *Phys. Rev. B* **107**, L020201 (2023).
- [25] J. F. Karcher, I. A. Gruzberg, and A. D. Mirlin, Generalized multifractality in two-dimensional disordered systems of chiral symmetry classes, *Phys. Rev. B* **107**, 104202 (2023).
- [26] I. Mondragon-Shem, T. L. Hughes, J. Song, and E. Prodan, Topological Criticality in the Chiral-Symmetric AIII Class at Strong Disorder, *Physical Review Letters* **113**, 046802 (2014).
- [27] J. Claes and T. L. Hughes, Disorder driven phase transitions in weak aiii topological insulators, *Phys. Rev. B* **101**, 224201 (2020).
- [28] Z. Xiao, K. Kawabata, X. Luo, T. Ohtsuki, and R. Shindou, Anisotropic Topological Anderson Transitions in Chiral Symmetry Classes, *Physical Review Letters* **131**, 056301 (2023).
- [29] P. Zhao, Z. Xiao, Y. Zhang, and R. Shindou, Topological effect on the anderson transition in chiral symmetry classes, *Phys. Rev. Lett.* **133**, 226601 (2024).
- [30] I. Herbut, *A Modern Approach to Critical Phenomena* (Cambridge University Press, 2007).
- [31] A. Tanaka and S. Takayoshi, A short guide to topological terms in the effective theories of condensed matter, *Science and Technology of Advanced Materials* **16**, 014404 (2015).
- [32] M. P. A. Fisher, P. B. Weichman, G. Grinstein, and D. S. Fisher, Boson localization and the superfluid-insulator transition, *Phys. Rev. B* **40**, 546 (1989).
- [33] L. Fallani, J. E. Lye, V. Guarrera, C. Fort, and M. Inguscio, Ultracold atoms in a disordered crystal of light: Towards a bose glass, *Phys. Rev. Lett.* **98**, 130404 (2007).
- [34] J. yoon Choi, S. Hild, J. Zeiher, P. Schauß, A. Rubio-Abadal, T. Yefsah, V. Khemani, D. A. Huse, I. Bloch, and C. Gross, Exploring the many-body localization transition in two dimensions, *Science* **352**, 1547 (2016).
- [35] R. B. Griffiths, Nonanalytic behavior above the critical point in a random ising ferromagnet, *Phys. Rev. Lett.* **23**, 17 (1969).
- [36] A. J. Bray, Nature of the griffiths phase, *Phys. Rev. Lett.* **59**, 586 (1987).
- [37] D. S. Fisher, Random transverse field ising spin chains, *Phys. Rev. Lett.* **69**, 534 (1992).
- [38] T. Vojta, Rare region effects at classical, quantum and nonequilibrium phase transitions, *Journal of Physics A: Mathematical and General* **39**, R143 (2006).
- [39] F. Vazquez, J. A. Bonachela, C. López, and M. A. Muñoz, Temporal griffiths phases, *Phys. Rev. Lett.* **106**, 235702 (2011).
- [40] M. Kiometzis, H. Kleinert, and A. M. J. Schakel, Dual description of the superconducting phase transition, *Fortschritte der Physik/Progress of Physics* **43**, 697 (1995).
- [41] M. Kiometzis, H. Kleinert, and A. M. J. Schakel, Critical

- exponents of the superconducting phase transition, *Phys. Rev. Lett.* **73**, 1975 (1994).
- [42] J. M. Kosterlitz and D. J. Thouless, Ordering, metastability and phase transitions in two-dimensional systems, *Journal of Physics C: Solid State Physics* **6**, 1181 (1973).
- [43] J. M. Kosterlitz, The critical properties of the two-dimensional xy model, *Journal of Physics C: Solid State Physics* **7**, 1046 (1974).
- [44] V. L. Berezinskii, Destruction of long-range order in one-dimensional and two-dimensional systems having a continuous symmetry group i. classical systems, *Soviet Journal of Experimental and Theoretical Physics* **32**, 493 (1971).
- [45] V. L. Berezinskii, Destruction of long-range order in one-dimensional and two-dimensional systems having a continuous symmetry group ii. classical systems, *Soviet Journal of Experimental and Theoretical Physics* **34**, 610 (1972).
- [46] R. Savit, Vortices and the low-temperature structure of the $x - y$ model, *Phys. Rev. B* **17**, 1340 (1978).
- [47] S. R. Shenoy, Vortex-loop scaling in the three-dimensional xy ferromagnet, *Phys. Rev. B* **40**, 5056 (1989).
- [48] E. Fradkin, B. A. Huberman, and S. H. Shenker, Gauge symmetries in random magnetic systems, *Phys. Rev. B* **18**, 4789 (1978).
- [49] J. V. José, L. P. Kadanoff, S. Kirkpatrick, and D. R. Nelson, Renormalization, vortices, and symmetry-breaking perturbations in the two-dimensional planar model, *Phys. Rev. B* **16**, 1217 (1977).
- [50] J. Cardy, *Scaing and Renormalization in Statistical Physics* (Cambridge University Press, Cambridge, 1996).
- [51] D. R. Nelson and D. S. Fisher, Dynamics of classical XY spins in one and two dimensions, *Phys. Rev. B* **16**, 4945 (1977).
- [52] G. A. Williams, Vortex dynamics and superfluid relaxation near the ^4He λ transition, *Phys. Rev. Lett.* **71**, 392 (1993).
- [53] G. A. Williams, Vortex-loop phase transitions in liquid helium, cosmic strings, and high- T_c superconductors, *Phys. Rev. Lett.* **82**, 1201 (1999).
- [54] G. A. Williams, Vortex fluctuations in the critical casimir effect of superfluid and superconducting films, *Phys. Rev. Lett.* **92**, 197003 (2004).
- [55] N. D. Antunes and L. M. A. Bettencourt, The length distribution of vortex strings in $U(1)$ equilibrium scalar field theory, *Phys. Rev. Lett.* **81**, 3083 (1998).
- [56] N. D. Antunes, L. M. A. Bettencourt, and M. Hindmarsh, Thermodynamics of cosmic string densities in $u(1)$ scalar field theory, *Phys. Rev. Lett.* **80**, 908 (1998).
- [57] K. G. Wilson and M. E. Fisher, Critical exponents in 3.99 dimensions, *Phys. Rev. Lett.* **28**, 240 (1972).
- [58] K. G. Wilson and J. Kogut, The renormalization group and the ϵ expansion, *Physics Reports* **12**, 75 (1974).
- [59] J. D. Jackson, *classical Electrodynamics (Third Edition)* (Wiley, 1999).